THE REGULATION AND FUNCTION OF LONG-CHAIN ACYL-COA DEHYDROGENASE AND THE EFFECT OF THE SINGLE NUCLEOTIDE POLYMORPHISM K333Q

by

Megan Elizabeth Beck

BS in Biology, Indiana University, 2008

MPH, University of Pittsburgh, 2012

Submitted to the Graduate Faculty of

Graduate School of Public Health in partial fulfillment

of the requirements for the degree of

Doctor of Philosophy

University of Pittsburgh

2016

UNIVERSITY OF PITTSBURGH

GRADUATE SCHOOL OF PUBLIC HEATH

This dissertation was presented

by

Megan Elizabeth Beck

It was defended on

June 3, 2016

and approved by

David N. Finegold, MD, Professor, Pediatrics, School of Medicine and
Human Genetics, Graduate School of Public Health, University of Pittsburgh

Candace M. Kammerer, PhD, Associate Professor, Human Genetics
Graduate School of Public Health, University of Pittsburgh

Gerard Vockley, MD PhD, Professor, Pediatrics, School of Medicine and
Human Genetics, Graduate School of Public Health, University of Pittsburgh

Dissertation Advisor: Eric S. Goetzman, PhD, Assistant Professor, Cell Biology &
Molecular Physiology, Interdisciplinary Biomedical Graduate Program and
Research Assistant Professor, Human Genetics
Graduate School of Public Health, University of Pittsburgh

Eric S. Goetzman, Ph.D

THE REGULATION AND FUNCTION OF LONG-CHAIN ACYL-COA DEHYDROGENASE AND THE EFFECT OF THE SINGLE NUCLEOTIDE POLYMORPHISM K333Q

Megan Elizabeth Beck, PhD

University of Pittsburgh, 2016

ABSTRACT

Nine acyl-CoA dehydrogenases (ACADs) are involved in mitochondrial fatty acid β-oxidation (FAO), an important energy-producing pathway. Disorders of FAO are common inborn errors of metabolism and genetic deficiencies have been identified for all ACADs except long-chain acyl-CoA dehydrogenase (LCAD). Understanding the function of LCAD and the phenotype of LCAD deficiency may enable identification of unrecognized cases of LCAD deficiency, and eventual treatment, and improve public health.

I hypothesized that human LCAD (hLCAD) and mouse LCAD (mLCAD) are biochemically equivalent, but that hLCAD functions in tissues not normally reliant upon FAO, such as the lung. Additionally, I hypothesized that a missense polymorphism (K333Q), linked to an absence of LCAD antigen in human lung, is deleterious. Recombinant mLCAD, hLCAD, and hLCAD K333Q proteins were purified and biochemically characterized. Recombinant mLCAD was more stable and demonstrated higher catalytic efficiency than hLCAD. Additionally, recombinant hLCAD bearing the K333Q substitution demonstrated lower activity, impaired substrate binding, and reduced stability compared to wild-type hLCAD.

Based on these findings and on western blotting experiments demonstrating higher LCAD expression in human lung than other long-chain ACAD enzymes, I hypothesized that

LCAD K333Q may be associated with lung disease. Primary alveolar type II (ATII) cells from individuals homozygous for the minor Q allele had five-fold less LCAD antigen than ATII cells from individuals homozygous for the major K allele, consistent with lower protein stability. Cohorts of neonates with respiratory distress syndrome and children hospitalized for pneumonia were genotyped for LCAD K333Q. Association of lung function with different genotypes at the K333Q locus was examined in the Long Life Family Study (LLFS) (N=4953). Contrary to the hypothesis, the LCAD K333Q locus was not associated with lung disease. Heterozygotes for the Q allele were under-represented among children hospitalized with pneumonia, whereas homozygotes for the K allele were over-represented, suggesting that carrier status for K333Q confers some benefit. Individuals in the LLFS who carried the Q-allele at the K333Q locus had increased lung function. In conclusion, recombinant mLCAD was biochemically superior to hLCAD, which was superior to hLCAD K333Q. However, the K333Q polymorphism was not associated with respiratory distress or pneuomonia-induced complications.

TABLE OF CONTENTS

LIST OF TABLES

LIST OF FIGURES

ACKNOWLEDGMENTS

I am deeply grateful to many people who supported my directly and indirectly in this research. I would like to first thank my mentor, Dr. Eric Goetzman, for his indispensable expertise, guidance, and support in concluding this project. I would also like to particularly thank Dr. David Finegold, Dr. Candace Kammerer, and Dr. Jerry Vockley for generously serving on my thesis committee, for their support, and for their highly valuable guidance of this research.

I would like to thank the members of the Goetzman Lab. I am very grateful for the friendship and support of Yuxun Zhang, Sivakama Bharathi, and Radha Uppala over the years of this project. I am grateful to Dr. Al-Walid Mohsen for his expertise in ETF preparation, particular assistance in analyzing a crystal structure, and expertise in enzymology. I would like to thank the members of the Vockley lab for their kindness and support during this research. In particular I am especially grateful for their generous time, assistance, and for providing humor and enjoyment in the group work of preparing ETF from pig livers.

Many collaborators generously provided materials and support. I am incredibly grateful to the Vockley lab for the kind gift of antibodies for western blot, to Dr. Eric Goetzman and Dr. Chikara Otsubo for their provision of BALF and lung tissue from LCAD -/- and Wt mice and the infection of LCAD -/- and Wt mice with influenza, to Dr. John Alcorn for the analysis of the pathology of the lungs of mice infected with influenza, to Dr. Jatinder Singh and Dr. Candace Kammerer for their analysis of the Long Life Family Study, to Dr. Beata Kosmider and Dr. Jieru

Wang at Jewish National in Denver, Colorado and the University of Pittsburgh for their gifts of DNA and primary ATII cell lysates from lungs not suitable for transplantation, to Dr. Mary Dahmer and her lab at the University of Michigan for the genotyping and analysis of 775 children hospitalized for pneumonia, to Dr. Larry Nogee at Johns Hopkins University for the DNA samples of children with respiratory distress syndrome, to Dr. to Dr. Edward Prochownik and Dr. Lia Edmonds for mouse hepatocyte lysates, to Dr. Henry Dong at the University of Pittsburgh for human hepatocyte lysates, and to Dr. Jung-Ja Kim at the Medical College of Wisconsin for providing the unpublished human LCAD crystal structure.

I am very thankful to the faculty and staff of the Graduate School of Public Health for their incredibly valuable training and support during my graduate student career at the University of Pittsburgh.

I am deeply indebted to my family for their love and support during these years of study and research.

I am incredibly thankful, and would not still be standing without my savior Jesus Christ.

Finally, I am thankful to the Research Advisory Committee (RAC) of UPMC Children's Hospital of Pittsburgh, PA who provided funding for this research through a RAC grant.

1.0 INTRODUCTION

1.1 FATTY ACID OXIDATION

Fatty acid oxidation (FAO) is the sequential cleavage of free acetyl-CoA groups from long-chain fatty acids to provide an important source of energy to support muscle activity, non-shivering thermogenesis, and liver function, particularly during illness, stress, and fasting (Vockley J. and Whiteman D.A.H 2002). Fatty acids are an important source of energy within tissues that require high amounts of energy: heart, brown adipose tissue, skeletal muscle, and liver (Goetzman E.S., 2011). Twenty-five proteins responsible for transport and enzymes are involved in FAO in the mitochondria. Defects in 88% of these proteins have been reported to cause disease (Vockley J. and Whiteman D.A.H. 2002). FAO begins with the conversion of fatty acyl-CoA substrates to acylcarnitines by the enzyme carnitine palmitoyltransferase-I (CPT1), a highly-regulated enzyme that serves as the "gatekeeper" for mitochondrial FAO. Acylcarnitines are transported through the outer and inner mitochondrial membranes and then converted back into acyl-CoAs in the mitochondrial matrix by carnitine palmitoyltransferase-2 (CPT2). The carnitine shuttle has great clinical relevance in FAO disorders. In the face of accumulating acyl-CoAs, which tie up the intra-mitochondrial CoA pool, CPT2 can catalyze the reverse reaction, resulting in efflux of acylcarnitines from the mitochondria. These acylcarnitines then accumulate

in blood where they are diagnostic for FAO disorders, and are the basis of newborn screening programs for these diseases (Moczulski D., et al. 2009).

Once inside the matrix, long-chain acyl-CoAs are processed through four steps of β-oxidation in which an acetyl-CoA is produced through the cleaving of two carbons from the fatty acid. These four steps include dehydrogenation, hydration, another dehydrogenation, and finally a thiolytic cleavage (Moczulski D., et al. 2009). The first step of dehydrogenation is the creation of a trans-α,β double bond through the action of acyl-CoA dehydrogenase enzymes (Chegary M., et al. 2009), with concomitant transfer of electrons to electron transfer flavoprotein (ETF) (Roberts D.L., et al. 1996). ETF Dehydrogenase oxidizes the reduced ETF, the electrons are then passed to coenzyme Q, and finally to complex III where it can go through the mitochondrial respiratory chain to produce ATP (Goetzman E.S., 2011) (Ruzicka F.J. and Beinert H. 1977). The second step of FAO is the hydration of 2-enoyl-CoA to 3-hydroxyacyl-CoA. The third step is the creation of 2-ketoacyl-CoA through 2,3 dehydrogenation of 3-hydroxyacyl-CoA. This dehydrogenation is reliant on NAD+ as a cofactor. The fourth and final step is the production of acetyl-CoA and an acyl-CoA that has been shortened in length by two carbons through the cleaving of the thioester bond by a thiolase. The shortened acyl-CoA can begin the cycle again at the first step of β-oxidation to cleave another acetyl-CoA.

The FAO pathway functionally interacts with the TCA cycle and the electron transport chain at multiple points (Figure 1). First, each FAO cycle directly produces NADH and $FADH_2$ that are sent to the respiratory chain to be oxidized and produce ATP. Second, the acetyl-CoA produced by β-oxidation can be subsequently oxidized to completion by the TCA cycle, further producing NADH and $FADH_2$ that is then sent to the mitochondrial respiratory chain (Moczulski D., et al. 2009).

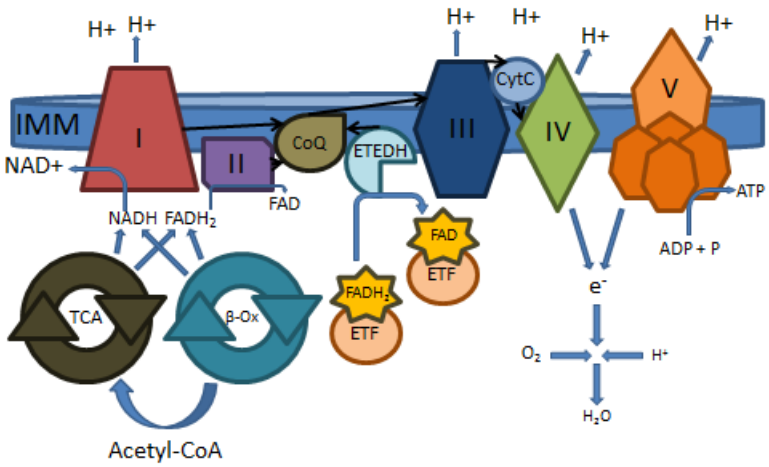

Figure 1: Interaction of B-Oxidation, TCA Cycle, and Respiratory Chain

1.2 ACYL-COA DEHYDROGENASE ENZYMES

1.2.1 Acyl-CoA dehydrogenase (ACAD) family members and substrate specificity.

The first dehydrogenation step in FAO is executed by the family of ACAD enzymes. There are 9 confirmed ACAD enzymes (Swigoňová Z., et al. 2009). Five of these enzymes play a role in FAO by catalyzing the production of *trans*-enoyl-CoA through the α,β-dehydrogenation of substrates: short-chain acyl-CoA dehydrogenase (SCAD), medium-chain acyl-CoA dehydrogenase (MCAD), long-chain acyl-CoA dehydrogenase (LCAD), very long-chain acyl-CoA dehydrogenase (VLCAD), and acyl-CoA dehydrogenase 9 (ACAD9). As suggested by their names, these five enzymes have differing substrate specificities. SCAD is active against short-chain acyl-CoAs 4 to 6 carbons in length, while MCAD oxidizes fatty acids of 6 to 16 carbons in length (Finocchiaro G., et al. 1987). VLCAD is active against acyl-CoAs of 14 to 20 carbons (Souri M., et al. 1998). There are two isoforms of VLCAD, dubbed the long and short

forms, due to alternative splicing of exon 3 (Goetzman E.S., et al. 2007). ACAD9 oxidizes fatty acids of approximately 10 carbons to about 18 carbons, but has even greater activity toward unsaturated fatty acids with the highest activity toward *cis*-9-$C_{16:1}$-CoA (He M., et al. 2007) (Zhang J., et al. 2002) (Ensenauer R., et al. 2005). Finally, LCAD has broad substrate specificity, exhibiting overlap with MCAD, VLCAD, and ACAD9, in that it demonstrates activity against saturated and unsaturated acyl-CoAs from 8 to 18 carbons as well as branched-chain acyl-CoAs (Le W., et al. 2000).

Four ACAD enzymes play roles in amino acid catabolism: isovaleryl-CoA dehydrogenase (IVD) has enzymatic activity toward leucine, short/branched-chain acyl-CoA dehydrogenase or additionally known as 2-methyl branched-chain acyl-CoA dehydrogenase (SBCAD) catabolizes isoleucine, isobutyryl-CoA dehydrogenase (IBD) catabolizes valine, and glutaryl-CoA dehydrogenase (GCD) catabolizes lysine and tryptophan (Swigoňová Z., et al. 2009). Two additional ACADs, acyl-CoA dehydrogenase 10 (ACAD10) and acyl-CoA dehydrogenase 11 (ACAD11), have been reported. The specific enzymatic activity of those ACADs has yet to be confirmed. However, the sequences of these proteins are homologous to the other ACADs (Swigoňová Z., et al. 2009). The ACAD enzymes are encoded in the nucleus. The precursor proteins are synthesized in the cytosol, transported into the mitochondria, and finally processed through a proteolytic mechanism into mature forms (Swigoňová Z., et al. 2009) (Goetzman E.S., 2011). All ACADs, as well as their redox partner ETF, are flavoproteins that incorporate a non-covalently bound flavin adenine dinucleotide (FAD) (Wanders R.J., et al. 1999) (Goetzman E.S., 2011) (Swigoňová Z., et al. 2009) during protein folding inside the mitochondrial matrix (Goetzman E.S., 2011).

1.2.2 **Structure of ACAD Enzymes.**

SCAD, MCAD, IVD, IBD, SBCAD, GCD, and LCAD are homotetramers (Figure 2) (Toogood H.S., et al. 2006). On the other hand, the ACADs VLCAD and ACAD9 are homodimers (Figure 3) (Pike A.C.W., et al. 2007). Additionally, SCAD, MCAD, IVD, IBD, SBCAD, GCD as well as LCAD are found in the mitochondrial matrix. VLCAD and ACAD9 are bound to the mitochondrial membrane. The crystal structures of human VLCAD, MCAD, IVD, and IBD have been reported. The ACAD monomers consist of tertiary folds of an NH_2-terminal domain of α-helices, a COOH-terminal domain of α-helices, as well as a central domain of β-sheets. LCAD has no reported crystal structure. Each monomer contains a non-covalently bound FAD cofactor. The flavin moiety of an FAD is bound at the active site of a subunit between the central β-sheet and the α-helices of the carboxyl terminus whereas the adenine moiety of the same FAD cofactor is bound between the α-helices of the carboxyl terminus of the adjacent subunit (Swigoňová Z., et al. 2009). Each ACAD has a spectrum including a peak of absorbance near 280nm as well as a peak near 445nm (Mohsen A.-W. and Vockley J. 2015). ETF is responsible for the transfer of electrons during the enzymatic activity of ACADs. Crystal structure analysis of MCAD shows a complex of MCAD with ETF through about 10 arginine residues as well as six histidine residues (Parker A.R., 2003). All ACADs have been shown to have a glutamic acid as the catalytic base responsible for initiating dehydrogenation of α-proton-abstracting. The location of the catalytic base is E376 in SCAD as well as MCAD. However, the location of the catalytic base is not conserved in LCAD, but is instead E261 (Djordjevic S., et al. 1994).

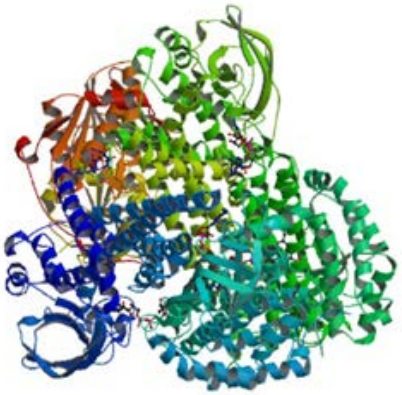

Figure 2: Crystal Structure of a Homotetramer of Human MCAD (pdb 1T9G)

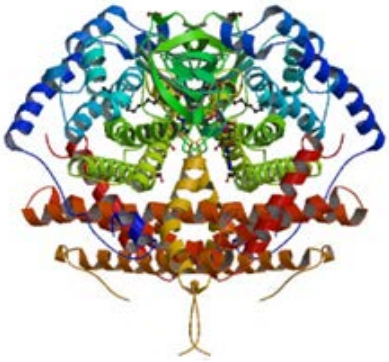

Figure 3: Crystal Structure of a Homodimer of Human VLCAD (pdb 2UXW)

1.2.3 Human ACAD Enzyme Deficiencies and Public Health Significance

FAO in the mitochondria provides maintenance of energy homeostasis during conditions of stress or fasting (Chegary M., et al. 2009). Genetic diseases have been associated with the dysfunction of at least 22 of the 25 enzymes that are known to play a role in mitochondrial FAO (Vockley J. and Whiteman D.A.H. 2002). For the ACAD enzyme family, genetic deficiencies have been noted for eight out of the nine bona fide ACADs, with LCAD being the only

exception. However, as a group, genetic disorders of FAO are the most common inborn errors of metabolism (Chegary M., et al. 2009). Inborn errors of FAO are estimated to contribute to up to 5% of sudden unexplained infant death (Moczulski D., et al. 2009). Therefore, understanding as well as treating disorders of FAO is of great public health significance.

The most common disorder of FAO is Medium-Chain Acyl-CoA Dehydrogenase Deficiency (MCADD), which is seen in about 1 out of every 15,001 births (Andresen B.S., et al. 2001). The symptoms of this most common disorder of FAO begin in early childhood after decreased intake of dietary carbohydrates concurrent with illness or fasting. The symptoms include vomiting, lethargy, hypotonia, possible mild hepatomegaly, seizures, hypoglycemia, hyperammonemia, and increased liver enzymes. The symptoms range from early hypoglycemia in newborns to asymptomatic. Prior to the development of successful newborn screening by tandem mass spectrometry to facilitate the diagnosis of MCADD, about 25% of the patients died due to their first episode (Wanders R.J., et al. 1999) (Wilcken B., et al. 1994). Treatment of MCADD involves the rapid treatment of episodes with hydration, glucose given intravenously, L-carnitine may be given intravenously when it is not possible to give it enteral or if the episode is severe. The current treatment to prevent episodes is the avoidance of fasting (Moczulski D., et al. 2009).

Another inborn error of FAO is SCAD deficiency. The prevalence of SCADD is estimated to be approximately 1 out of 50,000 births. The phenotype of SCAD deficiency (SCADD) manifests a variety of symptoms including metabolic acidosis, ketotic hypoglycemia, development, failure to thrive, developmental delay, seizures, and neuromuscular symptoms including myopathy and hypotonia. The symptoms of SCADD typically decrease with age. Treatment of acute symptoms of SCADD includes intravenous high dextrose fluids as in other

disorders of FAO. Symptoms of SCADD might be prevented by avoiding fasting (Jethva R., et al. 2008).

Patients with a deficiency of ACAD9 demonstrate a variable phenotype with cardiomyopathy, episodic liver dysfunction during mild illness with ingestion of aspirin, as well as chronic neurological dysfunction. The substrate specificity of ACAD9 overlaps with VLCAD. However, VLCAD does not appear capable of compensating for the loss of ACAD9 (He M., et al. 2007). This observation may be explained by the discovery that ACAD9 has a role in the assembly of Complex I of the mitochondrial respiratory chain in addition to FAO. Therefore, both the loss of long-chain FAO as well as the assembly of Complex I may contribute to the symptoms of ACAD9 deficiency (Schiff M., et al. 2015).

Between 1985 and 1993, 13 patients were described with a long-chain FAO disorder that was ascribed to deficiency of LCAD. These patients were reported with symptoms of cardiomegaly, hepatomegaly, hypoketotic hypoglycemia, as well as muscle weakness. However, with the discovery of the VLCAD gene in 1993, patients who were previously reported as having LCADD were instead deficient in VLCAD protein (Yamaguchi S., et al. 1993). VLCAD Deficiency (VLCADD) manifests in patients with early onset cardiomyopathy and skeletal myopathy as well as hypoketotic hypoglycemia, hyperammonemia, dysfunction of hepatocytes, cardiac arrhythmia, rhabdomyolysis, and myopathy in adolescence (Vockley J. and Whiteman D.A.H. 2002) (Aoyama T., et al. 1995). The current treatment for VLCADD patients is the prevention of fasting, low fat diet, and supplementation of medium chain triglycerides (Tenopoulou M., et al. 2015). As of now, there are no reported patients with a deficiency of LCAD.

1.2.4 **Reversible post-translational lysine acetylation as a regulator of ACAD enzymes.**

In addition to being the "powerhouse" of the cell, mitochondria are involved in multiple signaling pathways including apoptosis (Papanicolaou K.N., et al. 2014). Therefore, the regulation of mitochondrial signaling pathways may have significant consequences to cellular function. Lysine acetylation of mitochondrial proteins, as well as other post-translational modifications, impacts the signaling pathways of the mitochondria. Complex changes of acetylation in the mitochondria have been correlated with altered substrate fluctuation during fasting and feeding (Papanicolaou K.N., et al. 2014). Acetyl-CoA, the product of FAO, is the acetyl group donor for lysine acetylation of mitochondrial proteins, including the ACADs and other members of the FAO enzymatic machinery (Papanicolaou K.N., et al. 2014). The acetylation of lysines can be reversed in an NAD+-dependent manner by the sirtuin (Sirt) family of lysine deacylase enzymes. Reversible lysine acetylation may play a role in the pathophysiology of FAO disorders. Importantly, our lab has previously shown that acetylation of two lysines in recombinant mouse LCAD, K318 and K322, reduces the enzymatic activity (Bharathi S.S., et al. 2013). Similarly, acetylation/succinylation of key lysine residues on VLCAD inhibits enzymatic activity and membrane localization (Zhang Y., et al. 2015). Removal of the acetyl groups by Sirt3 rescues the loss of the enzymatic activity (Bharathi S.S., et al. 2013). Interestingly, aspirin, which can trigger Reye-like symptoms and acute symptoms in patients with FAO disorders (Tein I., 2015) (He M., et al. 2007), has been shown to acetylate multiple cellular proteins (Wang J., et al. 2015). This process appears to occur via transfer of the acetyl group of acetylsalicylic acid (aspirin) directly to protein lysines (Wang J., et al. 2015). Thus, protein acetylation may contribute to aspirin-induced metabolic decompensation among patients with mutations in the FAO pathway.

1.3 LCAD: THE "ORPHAN" ACAD ENZYME

1.3.1 LCAD deficiency may present differently than other ACAD deficiencies

As detailed above, genetic diseases are associated with all ACAD enzymes except LCAD (Vockley J. and Whiteman D.A.H. 2002). There are three plausible explanations for the absence of patients with disease-causing mutations in LCAD. The first possible explanation is that LCADD is embryonic lethal. No live patients would then be found. Evidence to support this possibility comes from the LCAD knockout mouse model, which has reduced litter size due to early embryonic lethality (Berger P.S. and Wood P.A. 2004) (Kurtz D.M., et al. 1998). A second plausible explanation is that the phenotype of LCADD differs from known acyl-CoA dehydrogenase (ACAD) deficiencies, so the disease has not been recognized as an ACAD deficiency. For example, Roberts and colleagues suggested that LCAD deficiency may be associated with the development of autism (Roberts J.L., et al. 2014). Additionally, LCAD is the only long-chain ACAD that is appreciably expressed in the human lung, kidney, thyroid gland, and prostate (He M., et al. 2007). Our lab has demonstrated a role for LCAD in the production of surfactant in the lung, and identified cases of SIDS where no LCAD antigen was visible in lung tissue. LCAD knockout mice displayed altered lipid composition and function of pulmonary surfactant (Goetzman E.S., et al. 2014). This result indicates that a possible LCADD patient may present with symptoms very unlike those of a traditional long-chain FAO disorder such as VLCADD, which affects the heart, muscle, and liver (He M., et al. 2007). A final possible explanation may be that a loss of LCAD does not result in any phenotype, so there is no disease of LCADD. The central hypothesis of my thesis, which will be detailed in a subsequent

section, is that LCADD patients exist, but they manifest a different clinical picture than other ACAD deficiencies.

1.3.2 **Lessons from the LCAD knockout mouse model.**

An LCAD knockout mouse model was created in the laboratory of Dr. Philip Wood nearly 20 years ago. The phenotype of the LCAD knockout mouse consists of intolerance of cold and fasting, hypoketotic hypoglycaemia, fatty acid changes in liver and heart tissue, and even sudden death. This phenotype is strikingly similar to human VLCAD deficiency (Kurtz D.M., et al. 1998) (Van Viles N., et al. 2005). LCAD-/- mice also accumulate $C_{14:1}$-acylcarnitine, the hallmark biochemical marker for human VLCAD deficiciency, in blood and multiple tissues (Kurtz D.M., et al. 1998) (Cox K.B., et al. 2001)

LCAD has also been suggested to play a role in fat tissues. The hypothalamic-sympathetic network works in conjunction with brown adipose tissue and has a significant function in energy metabolism (Motyl K.J., et al. 2013). *Misty* mice have reduced brown adipose tissue function (Motyl K.J., et al. 2013). *Misty* mice have reduced baseline levels of LCAD, however, during exposure to cold *Misty* mice had elevated expression of genes, including LCAD, that are correlated with white adipose tissue transitioning toward brown adipose tissue (Motyl K.J., et al. 2013). In mice, a morphological alteration from white adipose cells to cells that resemble brown adipocytes with higher number of mitochondria has been reported to occur with an increased metabolic rate in white adipose tissues. Therefore, LCAD may play a role in regulating the transition of white fat to brown fat in order to provide the needed metabolism as well as heat energy. This could also be confirmed in the cold-intolerance of LCAD -/- mice (Guerra C., et al. 1998).

Why mitochondria possess both LCAD and VLCAD is not clear, because they have largely overlapping substrate specificities. In mice, LCAD is widely expressed and appears to play a dominant role over VLCAD in the FAO pathway. This conclusion is evidenced by a comparison of the LCAD and VLCAD knockout mouse models. Compared to either LCAD knockout mice or humans with VLCADD, the VLCAD knockout mouse model (VLCAD -/-) manifests a phenotype that is much more mild. Enzyme activity assays with LCAD-/- and VLCAD-/- liver homogenates indicated a more severe loss of total long-chain ACAD activity in the LCAD-/- strain. As a result, VLCAD -/- mice show only mild hepatic steatosis and mild fatty acid change in the heart, and only under the stress of extreme fasting or cold temperatures (Cox K.B., et al. 2001). In contrast, LCAD-/- mice develop much more severe hepatic steatosis and signs of cardiac involvement (Cox K.B., et al. 2001). Therefore, our understanding of the physiology of the mouse models of LCAD -/- and VLCAD -/- and their representation of the human diseases is incomplete.

1.3.3 LCAD Single Nucleotide Polymorphism, K333Q

The overall population frequency of a specific single nucleotide polymorphism (SNP) in LCAD (rs2286963) (LCAD K333Q) is estimated to range from 21.1% (1000 Genomes Project), to 30.1% in the Exome Aggregation Consortium (ExAC) (Lek M, et al., 2015), to 27.7% NHLBI Grand Opportunity Exome Sequencing Project (GO-ESP) (Exome Variant Server, 2016) (NCBI. dbSNP Short Genetic Variations, 2013). The minor allele frequency in specific populations ranges from 0.0471 in the Mende population in Sierra Leone to 0.3485 in Utah Residents (NCBI. 1000 Genomes Browser, 2013). The SNP LCAD K333Q is a missense mutation that changes a lysine to a glutamine (NCBI. dbSNP Short Genetic Variations, 2013), but it has not been

associated with a disease and is of unknown significance (NCBI. dbSNP Short Genetic Variations, 2013). However, the metabolite C9-carnitine is elevated in the blood of those with the LCAD K333Q (Illig T., et al. 2010). This metabolite is likely 2,6-dimethylheptanoyl-carnitine, which is one of the branched-chain acyl-carnitine species that is predicted to accumulate with the dysfunction of LCAD (Van Viles N., et al. 2005). Additionally, our lab found that two samples from infants who died from Sudden Unexplained Infant Death (SUID) that showed a lack of LCAD antigen by Western Blot analysis were homozygous for LCAD K333Q. A sample from a third infant who also died from SUID exhibited LCAD antigen and was heterozygous for LCAD K333Q (Goetzman E.S., et al. 2014).

LCAD K333Q was associated in a Geographic-wide Associated Study (GWAS) of the 52 populations within the Human Genome Diversity Project with UV radiation (Pearson R value of 0.813366; Hsu I., et al. 2013). The SNP was also associated with an increased waist circumference. However, when corrected for multiple testing with Bonferroni adjustments, the association was not significant (Banasik K., et al. 2011). LCAD K333Q is associated with an increase of the mRNA of ACADL in liver tissue, but again, this relationship was not significant ($P < 0.1$) (Mirkov S., et al. 2012). Additionally, no difference was found in LCAD antigen levels in the fibroblasts of Danish people who were homozygous wildtype, heterozygous, or homozygous for the polymorphism (Andresen B.S., et al. 1999).

1.4 HYPOTHESES AND SPECIFIC AIMS OF THIS STUDY

1.4.1 Human LCAD and mouse LCAD are functionally equivalent.

I hypothesized that human LCAD (hLCAD) and mouse LCAD (mLCAD) are functionally equivalent. This hypothesis was tested by comparing recombinant hLCAD to mLCAD in terms of a) substrate specificity, determined by measuring maximum activity of the recombinant enzymes across several different chain-length substrates; b) substrate binding, using an anaerobic substrate titration assay; c) stability; and d) catalytic efficiency, calculated from kinetic parameters obtained by enzyme activity assays. Further, the tissue expression of mLCAD and hLCAD were examined using western blot of human breast, kidney, liver, lung, pancreas, prostate, and thyroid tissue lysates and mouse kidney, liver, lung, and pancreas tissue lysates with LCAD antibodies. VLCAD, which has overlapping substrate specificity with LCAD, was also quantified (Souri M., et al. 1998) (Le W., et al. 2000).

1.4.2 The function of LCAD is regulated by post-translational modification.

Our lab has previously shown that acetylation of mLCAD at lysines 318 and 322 reduces the enzymatic activity (Bharathi S.S., et al. 2013), and that this can be reversed by the sirtuin deacylase enzyme SIRT3. Also, aspirin has recently been shown to acetylate cellular proteins, and historically aspirin has been recognized as a trigger of metabolic decompensation in patients with FAO disorders (Wang J., et al. 2015) (Tein I., 2015) (He M., et al. 2007). I hypothesized that aspirin may acetylate LCAD and reduced function. A human cell line was treated with aspirin and the resulting changes in hLCAD acetylation were measured. Finally, I examined

"global' protein lysine acetylation in primary human primary alveolar type II (ATII) cells, which have not previously been characterized for this post-translational modification, because our laboratory has previously identified the ATII cells as a site of high hLCAD expression (Goetzman E.S., et al. 2014).

1.4.3 The common polymorphism of LCAD K333Q has detrimental consequences, particularly in the lung.

As mentioned above, our laboratory has previously shown that lung ATII cells express high levels of hLCAD, and two cases of sudden infant death were identified with no LCAD antigen. Both were homozygous for missense polymorphism K333Q (Goetzman E.S., et al. 2014). Based on this observation, I hypothesized that LCAD K333Q is a detrimental amino acid substitution that would serve as a risk factor for lung disease. Recombinant hLCAD with the SNP K333Q in the sequence produces purified LCAD with wild type lysine changed to a glutamine in all monomers (hLCAD K333Q). I assessed the impact of the SNP K333Q on recombinant hLCAD function toward five different acyl-CoA substrates as well as kinetic parameters and catalytic efficiency. A substrate titration assay was also used to compare the abilities of recombinant hLCAD Wt and hLCAD K333Q to bind substrate. Then, I examined a possible association of LCAD K333Q with human lung disease, using cohorts of children with respiratory distress syndrome or hospitalized for pneumonia. Finally, I explored relationships between K333Q and measures of lung function in the Long Life Family Study (LLFS) database.

1.4.4 **LCAD has a role in the immune system, particularly in the lung.**

I also hypothesized that LCAD has a role in the immune system, particularly in the lung. Some data shows that the SNP K333Q appears to be beneficial. Therefore, it is suspected that a role of LCAD may be detrimental, and the reduction of the detrimental role through the SNP K333Q may be beneficial. I examine this hypothesis because ATII cells where LCAD is expressed are involved in the immune system in the lung. Additionally, the surfactant of LCAD -/- mice is abnormal and decreased in abundance, the lung function of LCAD -/- mice is reduced, and inflammation of LCAD -/- mice infected with influenza is significantly less than that of wild type mice. Therefore, data is obtained from the LLFS in measures of possible association of the SNP K333Q with aspects of the immune system: IL-6, white blood cell counts, and C-reactive protein. Additionally, surfactant protein-A (SP-A) is examined by western blot in lung tissue lysates as well as bronchial alveolar lavage fluid of LCAD -/- mice compared to wild type mice to examine the secretion of SP-A into the surfactant. SP-A is examined because it is expressed in ATII cells where LCAD is expressed and it has a role in the immune system.

2.0 MATERIALS AND METHODS

2.1 PURIFICATION OF RECOMBINANT LCAD ENZYMES AND NATIVE ETF

The aims of biochemically comparing mLCAD to hLCAD, and subsequently hLCAD to hLCAD K333Q, required purified recombinant LCAD proteins as well as purified native ETF to serve as the electron acceptor in enzyme activity assays. These protein reagents were prepared as described below.

2.1.1 Expression and purification of recombinant LCAD proteins.

An *E coli* expression system for His-tagged mLCAD was previously described by our laboratory (Bharathi S.S., et al. 2013). For hLCAD, the hLCAD K333Q cDNA was obtained from Dr. Jung-Ja Kim of the Medical College of Wisconsin and was inserted into the pTrcHis bacterial expression vector (Thermo Fisher Scientific) containing a C-terminal His-tag sequence. Bacterial expression of hLCAD K333Q produces monomers that all contain the change of a lysine to a glutamine at site 333. Site-directed mutagenesis was then used to convert the hLCAD K333Q construct to wild type hLCAD using the QuikChange II Site-Directed Mutagenesis Kit (Agilent Technologies). To verify the reversion to the wild type sequence, plasmid DNA was prepared from four colonies using the GenElute Plasmid Miniprep Kit (Sigma-Aldrich) and

examined by restriction enzyme digest using the restriction enzyme BamHI to release the plasmid insert (Figure 4).

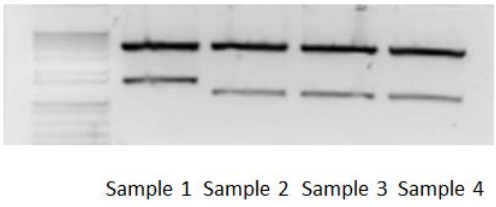

Figure 4: 1% Agarose Gel of BamHI Enzyme Digest of 4 Colonies from Q333K Mutagenesis

Samples 2, 3, and 4 appeared to be the correct size and were sent to GeneWiz (genewiz.com) for Sanger sequencing to confirm the reversion to the wild-type LCAD allele (Figure 5).

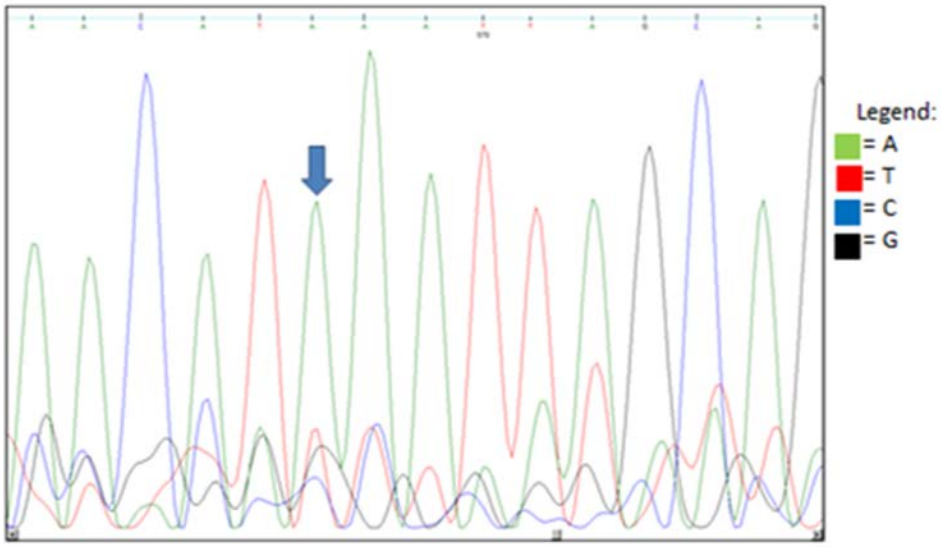

Figure 5: Sequence of Lysine 333 to Confirm Single Site Mutation of SNP Q to Wild Type K

All three recombinant LCAD proteins were expressed and purified in the same manner. Briefly, four-liter cultures of *E. coli* were induced overnight with 0.5 mM IPTG at 30 °C. The *E coli* cultures were pelleted and lysed by sonication (Fisher Scientific Sonic Dismembrator 550)

on ice in a cooling cell. Lysates were clarified by ultracentrifugation and the supernatants were applied to a 1 mL HisTrap column using an Amersham Pharmacia Biotech ÄKTA fast protein liquid chromatography (FPLC) system. Bound proteins were eluted with 50 mM $NaPO_4$, 100 mM NaCl, 10% glycerol, 300 mM Imidizole, pH8 with a linear gradient over 30 column volumes. Fractions containing LCAD were collected and dialyzed against 50mM NaPO4 pH 8, 50mM NaCl, 10% glycerol, 0.2 mM DTT, and then concentrated to greater than 3 mg/mL prior to flash-freezing in liquid nitrogen and subsequent storage at -80C. The purity of each protein preparation was examined by resolving 1 µg of protein on an SDS-page gel (Bio-Rad TGX) and staining with Coomassie (Figure 6).

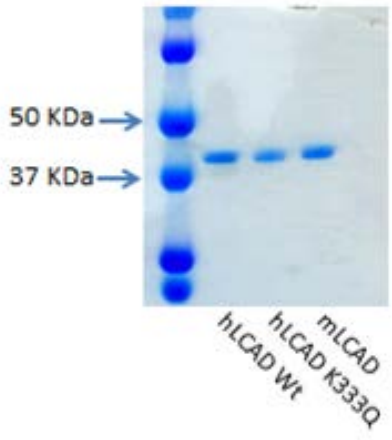

Figure 6: Coomassie Stain of 1 µg of Recombinant hLCAD Wt, hLCAD K333Q, and mLCAD on SDS Page Gel

The integrity of the purified hLCAD Wt and hLCAD K333Q proteins were determined by absorbance scanning and calculating the FAD ratio, defined as the ratio of total protein absorbance (A_{280}) to the FAD absorbance (A_{445}). LCAD is a homotetramer with an FAD cofactor non-covalently bound to each monomer; increased FAD ratios above 9 indicate partial loss of FAD from the tetramer. For all experiments involving, the proteins were purified in the

same manner as described above except when mentioned that 100 uM FAD was added to the dialysis and storage buffer. Before use, the excess unbound FAD was removed from the storage buffer using size exclusion columns (Bio-Rad Micro Bio-Spin ™ P-30) by exchanging the column buffer for dialysis buffer and using the columns according to manufacturer instructions.

2.1.2 **Purification of native porcine ETF.**

All ACAD enzymes use electron transferring flavoprotein (ETF), another flavoprotein, as their natural electron acceptor. For biochemical characterization of the three LCAD recombinant proteins, purified native porcine ETF protein was used as the electron acceptor in activity assays and kinetics experiments. Porcine ETF is used due to its high degree of intrinsic FAD-associated fluorescence, which becomes quenched as it accepts electrons from ACAD enzymes. To purify pig ETF, mitochondria were first isolated from freshly harvested pig liver. Briefly, pig liver was homogenized in 50 mM KPO_4, 1 mM EDTA, 2.5% glycerol, 250 mM sucrose, and the homogenate filtered through cheesecloth. The mitochondria were collected from the homogenate by a conventional differential centrifugation protocol, and mitochondrial pellets stored at -80 °C until time of ETF protein purification.

To purify ETF protein, approximately 500 g of frozen mitochondria were sonicated in an equal volume of 320 mM KPO_4, 10mM EDTA, 0.1 mg/mL FAD, and 0.2 mg/mL AMP (sonication buffer). The lysate was ultracentrifuged and the supernatant subjected to ammonium sulfate precipitation by adding powdered ammonium sulfate to 45% saturation. The sample was left to stir on ice for 10 minutes, then ultracentrifuged at 52,000 rpm for 35 minutes at 4 °C. The supernatant was collected, stirred on ice, and brought to 60% ammonium sulfate saturation. The ultracentrifuge step was repeated, and supernatant discarded. The pellet was resuspended in

sonication buffer, transferred to a dialysis bag, and dialyzed against 5 liters of 15 mM unbuffered K_2HPO_4 and 5% glycerol overnight, with three buffer changes.

Pig ETF was then purified using a series of chromatography steps on an FPLC system (Amersham Pharmacia Biotech ÄKTA). First, a negative chromatography step was employed using DEAE sepharose. ETF was recovered from the flow-through, easily recognized by its distinctive yellow color. Fractions containing ETF were pooled and subjected to chromatography on CM-Sepharose resin equilibrated with 10 mM Tris pH 8.5. After extensive washing, the ETF was recovered with a gradient from 0% to 100% 10 mM Tris with 100 mM NaCl pH 8.5. Fractions that fluoresced in ultraviolet light were collected and scanned on a spectrophotometer (Jasco V-650). The absorbance ratio A_{270}/A_{436} was calculated from the spectra to obtain the FAD ratio as an indicator of purity. Fractions with a ratio less than 7 were pooled as fraction A. Fractions with a ratio above 7 were pooled as fraction B. The pooled fractions were concentrated, the buffer was exchanged with 10mM Tris, and the samples flash frozen in liquid nitrogen and stored at -80 °C. The concentration of the stored protein was calculated using A_{436} (flavin peak) and the extinction coefficient of 0.0134.

2.2 BIOCHEMICAL COMPARISON OF RECOMBINANT LCAD PROTEINS

The biochemical evaluation of the three LCAD enzymes was conducted using four methodologies. First, steady-state enzyme activity was measured using the anaerobic ETF fluorescence reduction assay with saturating concentrations of various acyl-CoA substrates. Second, the same activity assay was used to determine catalytic efficiency by holding the amount of LCAD enzyme and ETF constant while varying substrate concentration. Third, the first half-

reaction (reductive) was followed by titrating the enzyme with substrates in the absence of the electron acceptor ETF. Finally, stability of the LCAD proteins was determined by exposing the recombinant proteins to different temperatures and monitoring the proteins by absorbance spectroscopy. These four techniques are described below.

2.2.1 LCAD steady-state enzyme activity assays.

The anaerobic ETF fluorescence reduction assay takes advantage of the fact that porcine ETF loses intrinsic fluorescence upon accepting electrons from ACAD enzymes. The assay is done under anaerobic conditions in sealed quartz cuvettes to eliminate secondary electron transfer to oxygen. The assay buffer (55 mM Tris-HCl pH 8) is supplemented with glucose (0.6%), glucose oxidase (≥ 180 units/mg protein), catalase (≥ 1000 units/mg protein), and warming the cuvette for at least 2 minutes such that O_2 is continually scavenged from the cuvettes. Additionally, each cuvette is cycled with argon gas and vacuum for several minutes after being sealed with a rubber stopper in order to remove as much O_2 as possible.

LCAD is thought to be active against a range of acyl-CoA substrates. Here, five substrates were used with chain lengths varying from 12 to 18 carbons, including one unsaturated substrate of 18 carbons that is physiologically relevant to FAO: C_{12}-CoA, C_{14}-CoA, C_{16}-CoA, C_{18}-CoA, and $C_{18:1}$-CoA, all from Sigma (St. Louis, MO). Substrate stocks were made in 2mM sodium acetate pH 5 and the concentration determined by dividing the A_{259} by the extinction coefficient (15.4). Working solutions (1 mM) were degassed just before the assay with alternating cycles of argon and vacuum. The assays were performed by adding enzyme (amount determined empirically for each LCAD enzyme, but usually about 100 -200 ng) and ETF (about 1 uM) to the cuvette needlewise. The reaction was started by injection of acyl-Co

substrate, and the change in fluorescence followed for 2 minutes on an FP-6300 Jasco spectrofluorometer excitation=340 nm, emission=490 nm). A typical reaction is illustrated in Figure 7. The slope of the initial reaction was taken as shown by the blue line in Figure 7 and used to calculate specific activity using the equation [(-52.75) x (slope/intercept) / (µg protein used/1000)]. Each cuvette was also measured in the absence of substrate to determine the background, which was negligible. For steady-state measurements, 25 uM substrate was used. The amount of LCAD enzyme was adjusted for each substrate such that the initial slope was kept to < 1.0, such that experimental error due to the time lag between injecting substrate and starting the data collection software (~3 sec) was kept to a minimum. All assays were measured in at least triplicate. Statistical analysis was done by a one-tailed Student's t-Test of two samples of unequal variance.

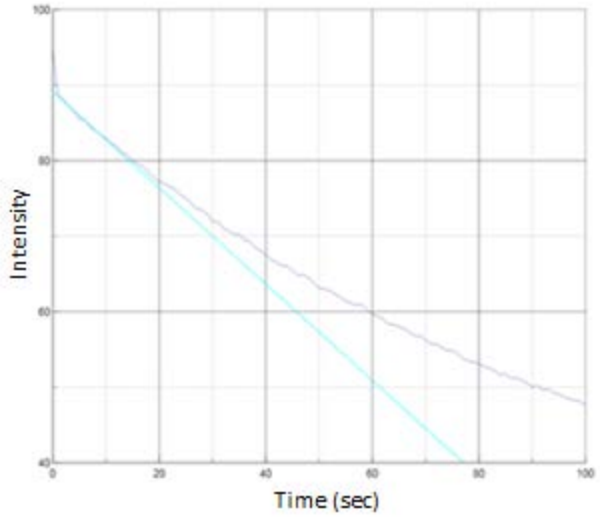

Figure 7: Time Course of Human LCAD Wt with ETF and Substrate on Spectrofluorometer

The recombinant protein examined with substrates C_{18}-CoA and $C_{18:1}$-CoA were stored in ACAD Dialysis Buffer with FAD, and prepared by removing the unbound FAD using size exclusion columns (Bio-Rad Micro Bio-Spin ™ P-30 Gel Columns in Tris Buffer) as per manufacture instructions.

2.2.2 LCAD enzyme kinetics.

A dilution series of C_{12}-CoA was prepared in 2 mM sodium acetate pH 5, which yielded a substrate concentration range of 0.575 to 73.6 μM final concentrations in the ETF fluorescence reduction assay. All substrate vials were degassed with alternating flows of argon and vacuum. Exogenous FAD was added to the LCAD enzymes with the storage buffer, any excess unbound FAD was removed using size exclusion columns (Bio-Rad Micro Bio-Spin ™ P-30 Gel Columns in Tris Buffer) as per manufacturer instructions.

Slopes and Y-intercepts were determined as in the steady-state assays for each recombinant enzyme with each of the concentrations of substrate, and activity calculated per μM of the electron acceptor ETF rather than per unit of LCAD enzyme using the equation: -((slope/intercept) / (μM ETF)) x (60/0.91). Each substrate concentration was assayed at least in triplicate. Then, Michaelis-Menten calculations were used (Graphpad Prism version 6.0) to determine the kinetic parameters of V_{max} and K_m for the curves of the enzymatic activity for each enzyme/substrate combination. Finally, catalytic efficiency was expressed per unit of LCAD-bound FAD to account for differences in FAD content between the various LCAD recombinant enzymes. FAD content of the specific aliquots of each recombinant LCAD used for kinetics were determined using FAD absorbance (A_{445}) and the extinction coefficient of 0.0139. The catalytic efficiency was calculated by using the equation $[(V_{max}/\text{FAD concentration})/60)/K_m]$.

2.2.3 **LCAD substrate titration assays (reductive half-reaction).**

Just as the ETF FAD loses fluorescence as it becomes reduced by accepting electrons, so does the FAD peak of each ACAD enzyme lose its absorbance (A_{445}). By titrating the recombinant LCAD enzyme with increasing amounts of substrate and measuring the responding loss of FAD absorbance, the rate of the reductive half-reaction (substrate binding and subsequent transfer of electrons to the FAD rings) can be followed. As with the ETF fluorescence reduction assay, substrate titrations were performed anaerobically to eliminate electron transfer to oxygen. After adding LCAD protein (1 mg/ml) in 500 µL of 25 mM potassium phosphate buffer, the cuvette was sealed, degassed and loaded into a spectrophotometer (Jasco V-650) blanked against 25 mM potassium phosphate. An initial spectra was taken from 200 nm to 800 nm, then 1 µL aliquots of a 1.66 µM substrate were injected, and a new spectra collected after each addition. The final substrate concentrations tested ranged from 0 to 48.35 uM. The absorbance data were processed by subtracting the absorbance at 800 nm from the absorbance peak at 443 nm (FAD) for each concentration of substrate, then normalizing to baseline (absence of substrate). The resulting FAD absorbance (A_{443}) values were plotted against substrate concentration in Graphpad Prism 6.0. Recombinant enzymes hLCAD Wt, hLCAD K333Q, and mLCAD were all titrated with C_{12}-CoA, while hLCAD Wt and hLCAD K333Q were further examined with C_{16}-CoA and C_{18}-CoA. The storage buffer of the enzyme titrated with C_{18}-CoA contained exogenous FAD. The unbound FAD was removed using size exclusion columns (Bio-Rad Micro Bio-Spin ™ P-30 Gel Columns in Tris Buffer) as per manufacturer instructions.

2.2.4 **Stability assays with recombinant LCAD proteins.**

An initial experiment was performed to test the stability by incubating recombinant proteins at 37 °C for 48 hours and measuring the absorbance of the samples from 200 nm to 800 nm using a spectrophotometer (Thermo Scientific NanoDrop 2000) at varying time points. However, an increase in absorbance near 345 nm was seen suggesting precipitation. Therefore, the experimental design was adjusted.

The absorbance of each protein sample from 200 nm to 800 nm was measured using a spectrophotometer (Thermo Scientific NanoDrop 2000) to obtain baseline data. Then, aliquots of protein were incubated for 30 minutes on ice, room temperature, 37 °C, and 55 °C. Every half hour for two hours, four microliters of each protein were removed, centrifuged at 14,000 rpm for 10 minutes at 20 °C to remove any precipitated material, and subjected to absorbance scanning from 200 nm to 800 nm. Then, the remainder of the samples were incubated overnight (19 hours). The samples were centrifuged for 10 minutes for 14,000 rpm at 20 °C and the spectra were measured using the supernatants. The stability was analyzed by measuring the peak of total protein near 280 nm to determine loss of protein due to precipitation at each temperature and time point.

2.2.5 **Rescuing recombinant LCAD with exogenous FAD.**

The cofactor FAD provides visible color to the purified proteins. However, recombinant hLCAD K333Q with a change from lysine to glutamine on all monomers is consistently more pale in color than recombinant hLCAD Wt. Therefore, a loss of FAD was examined by determining the FAD ratios of recombinant hLCAD WT and hLCAD K333Q as described

above. Furthermore, the rescue of any loss of FAD with exogenous FAD was examined. Purified recombinant proteins were incubated with a 100 µM concentration of FAD dissolved in purified water. The concentration of purified protein was measured using BCA assay. 163.7 µg of hLCAD Wt and K333Q were each diluted in separate tubes to 47 µL with ACAD Dialysis Buffer. A 100 µM final concentration of FAD dissolved in water was added to each tube. An amount of purified water equal to the volume of FAD added was added to separate samples of 163.7 µg hLCAD Wt and K333Q for control and all samples were incubated for 20 minutes at 37 °C. Unbound FAD was removed by passing all samples through size exclusion columns (Bio-Rad Micro Bio-Spin ™ P-30 Gel Columns in Tris Buffer) as described above. The activity of the protein was measured by performing ETF Assay with palmitoyl CoA as described above. Analysis of the enzymatic activity was done by a one-tailed Student's t-Test of two samples of unequal variance.

2.3 STRUCTURAL AND EXPRESSION DIFFERENCES BETWEEN MOUSE AND HUMAN LCAD

In addition to the biochemical comparison of hLCAD and mLCAD, experiments were performed to evaluate expression levels in various tissues not previously studied. For example, human heart and muscle have been reported to contain little or no LCAD protein. Here, I focused on liver, lung ATII cells, and other secretory epithelia similar to lung ATII cells (prostate, breast, etc). The levels of LCAD and VLCAD were determined to shed light on the relative roles of these two long-chain ACAD enzymes in human tissues. Further, I analyzed the amino acid sequences

of hLCAD and mLCAD to look for differences that might explain species differences in enzymatic activity. These methods are described in detail below.

2.3.1 Amino acid sequence alignment and three-dimensional structure analysis.

The amino acid sequences for the hLCAD and mLCAD were obtained from NCBI (ncbi.nlm.nih.gov/protein) (NCBI Protein, 2015) (NCBI Protein, 2006). Amino acid sequence alignment was performed using the program Blast (blast.ncbi.nlm.nih.gov/Blast.cgi) (NIH: NCBI, 2015). Species differences with regards to the FAD residues, substrate binding residues, and catalytic base were analyzed with the guidance of Dr. Al-Walid Mohsen on the three-dimensional human LCAD structure using the program Insight II (Accelrys, Inc 2005). The unpublished crystal structure for human LCAD was provided by Dr. Jung-Ja Kim (Medical College of Wisconsin).

2.3.2 Tissue expression of mouse versus human LCAD and VLCAD.

I first performed a screen of LCAD and VLCAD protein levels in various human tissue lysates. Human tissue lysates of normal breast, kidney, liver, lung, pancreas, prostate, and thyroid were obtained from G-Biosciences, prepared by reconstituting in 30 µL nuclease free H_2O to create a concentration of 5 µg/µL, and stored at -80 °C until use. Kidney, liver, lung, and pancreas were collected from a C57BL/6J wild type mouse. The tissues were homogenized in RIPA Buffer (Pierce) with protease inhibitors (Roche cOmplete, Mini) and phosphatase inhibitors (Boston BioProducts Phosphatase Inhibitors Cocktail-II). Fifty µg of each tissue lysate were resolved on an SDS page gel (Bio-Rad TGX) and transferred onto a nitrocellulose membrane (Bio-RAD,

0.45 μm). The membrane was blocked with 5% milk in TBS with 1% Tween-20 (TBS-T) for 1 hour at room temperature, and then LCAD and VLCAD were visualized using primary rabbit anti-sera (kind gift of Dr. Jerry Vockley) at 1:2500 followed by chicken anti-rabbit antibody IgG-HRP (Santa Cruz Biotechnology, 1:5000) and chemiluminsence western blotting substrate (Pierce).

2.3.3 Abundance of LCAD and VLCAD in human and mouse hepatocytes.

The relative abundance of LCAD and VLCAD in liver was further evaluated using primary murine and human hepatocytes (gifts of Dr. Lia Edmunds with Edward Prochownik, and Dr. Henry Dong respectively). Hepatocyte cell pellets were lysed by sonication in RIPA buffer (Pierce) with protease inhibitors (Roche cOmplete, Mini). Known amounts of recombinant LCAD and VLCAD proteins were mixed and used to create a dilution series that was loaded alongside the hepatocyte lysates as a standard curve. Following SDS-PAGE and transfer to nitrocellulose, the membrane was cut and the upper and lower pieces immunoblotted for VLCAD (subunit molecular weight of 68 kDa) and LCAD (subunit molecular weight of 42 kDa), respectively.

Additionally, the lower portion of the membrane was stripped (Restore ™ PLUS, Thermo Scientific) according to manufacturer instructions and immunoblotted for β-actin (Proteintech, IRP-labeled ACTB Monoclonal,1:20,000) as a loading control.

The program Image J was used to perform densitometry to create the standard curve of known concentration of recombinant proteins and determine the unknown concentrations of LCAD and VLCAD in the hepatocyte lysates. Statistical analysis was done by a one-tailed Student's t-Test of two samples of unequal variance.

2.4 LYSINE ACETYLATION OF HUMAN LCAD

Mouse LCAD is known to be subject to regulation by reversible lysine acetylation and the sirtuin enzyme SIRT3 (Bharathi S.S., et al. 2013). Nothing is known about the effects of lysine acetylation on hLCAD. This was investigated using two methodologies as described below.

2.4.1 Effects of chemical acetylation on recombinant hLCAD protein.

Maximal lysine acetylation of purified recombinant hLCAD proteins was achieved as our laboratory previously reported for purified recombinant mLCAD (Bharathi S.S., et al. 2013). Briefly, approximately 100 µg of recombinant hLCAD Wt and recombinant hLCAD K333Q with a change from lysine to glutamine on all monomers were incubated with 15 mM sulfo-NHS acetate (Thermo Scientific) in 50 mM KPO_4 pH 8 at room temperature for 1 hour. Mock-treated proteins served as control. The acetylation reaction was neutralized by adding 5 µL of 1 M Tris pH 8. Both the treated and mock-treated samples were dialyzed overnight in 20 mM Tris buffer pH 7.5 at 4 °C. The dialyzed proteins were functionally assessed using the anaerobic ETF fluorescence reduction assay with palmitoyl CoA as substrate, as described above. Statistical analysis of the enzymatic activity was done by a one-tailed Student's t-Test of two samples of unequal variance. Triplicates of the recombinant proteins for treated and mock-treated conditions were assessed for FAD ratio through spectroscopy as described above. Statistical analysis was done by a one-tailed Student's t-Test of two samples of unequal variance.

2.4.2 **Acetylation of hLCAD by aspirin in cultured cells.**

Aspirin, long known as a trigger of metabolic decompensation in patients with inborn errors of FAO (Tein I., 2015) (He M., et al. 2007), can chemically acetylate cellular proteins via its acetyl moiety (Wang J, et al. 2015). To test the effects of aspirin on hLCAD, HEK293 cells were transfected with a Flag-tagged hLCAD expression construct using Lipofectamine reagent (Thermo Fisher Scientific). The following day, half of the transfected cells were treated with a stock of aspirin dissolved in ethanol to a final aspirin concentration of 5 mM. After 24 hrs, aspirin-treated and untreated control cells were harvested, lysed in RIPA buffer (Pierce) with protease inhibitors (Roche cOmplete Mini), centrifuged at 16,100 x g for 15 minutes at 4 °C, and the supernatant collected. Immunoprecipitation using anti-Flag antibody was performed as follows. First, lysates were pre-cleared by incubating with Protein A agarose for 1 hour at 4 °C. The beads were pelleted by centrifugation and discarded. Then, the supernatant was mixed with 5 µg of anti-Flag primary monoclonal antibody M2 (Sigma-Aldrich) and rotated at 4 °C for 1 hour, followed by incubation with Protein A agarose for 2 hours at 4 °C. The agarose beads were pelleted, the supernatant removed and discarded, and the beads washed a total of four times in RIPA Buffer (Pierce). Finally, hLCAD-Flag was eluted by heating in Laemmli buffer at 80 °C for 10 minutes. The beads were removed by centrifugation and the supernatant subjected to immunoblotting with anti-acetyl-lysine antibody (Cell Signaling Technologies, 1:2,500) as the primary antibody and goat anti-mouse IgG-HRP (Santa Cruz Biotechnology, 1:5,000 as the secondary antibody. Following exposure to film, the membrane was stripped as described above and probed for LCAD antigen as a loading control. The program Image J was used to perform densitometry in triplicate for the untreated and aspirin treated samples. Statistical significance was calculated by a one-tailed Student's t-Test of two samples of unequal variance.

2.5 CORRELATION OF LCAD SNP K333Q WITH HUMAN LUNG PHENOTYPES

A high-throughput qPCR-based assay (Taqman, Applied Biosystems) for genotyping the hLCAD missense SNP K333Q was validated as described below, and then applied to cohorts of children with lung disease. Additionally, the correlation of K333Q with lung function indicators in the elderly was explored by mining the database from the Long Life Family Study (LLFS). Finally, the effect of SNP K333Q on antigen levels *in vivo* was determined using primary human ATII cells isolated from lungs that were genotyped for the SNP.

2.5.1 K333Q SNP genotyping assay and correlation with childhood lung phenotype.

First, 149 DNA samples from human lungs not suitable for transplantation were obtained from Dr. Beata Kosmider (Jewish National, Denver, CO) and used to optimize the Taqman SNP genotyping assay (Applied Biosystems) for LCAD K333Q. As control, two samples of lung DNA that had been genotyped by traditional Sanger Sequencing of exomes by GENEWIZ LLC were included. TaqMan ® Genotyping Master Mix, MicroAmp ® Fast Optical 96-well plates, and optical adhesive film were obtained from Applied Biosystems. Blank wells were prepared using water in place of template, while sample wells received approximately 10 ng of human genomic DNA. The plates were sealed, centrifuged briefly to eliminate air bubbles, and subjected to thermal cycling on a StepOnePlus Real-Time PCR thermal cycler (Applied Biosystems). The program consisted of 95 °C for 10 minutes followed by 40 cycles of 95 °C for 15 seconds and 60 °C for 1 minute. The genotypes were called using the StepOne software. Both controls were genotyped in agreement with the previous results and the 149 lung DNA samples yielded allele frequencies that were statistically similar to expected values based on

online SNP databases. The expected allele frequencies were determined from the general population based in the 1000 Genomes Project (NCBI. 1000 Genomes Browser, 2013). Statistical significance was calculated by a chi-squared test.

Next, DNA samples from 142 full-term or near full-term Caucasian neonates with respiratory distress syndrome were obtained from Dr. Larry Nogee (Johns Hopkins University) and genotyped with the Taqman assay described above. An additional 60 cases of respiratory distress and age-matched controls were genotyped by Dr. Jennifer Wambach at Washington University. Finally, 775 children (474 African American and 301 Caucasian) hospitalized for pneumonia were genotyped by Dr. Mary Dahmer at the University of Michigan using our reagents and protocol. The expected allele frequencies were determined from the allele frequencies of Caucasian Utah residents and Americans of African Descent based in the 1000 Genomes Project (NCBI. 1000 Genomes Browser, 2013). Statistical significance was calculated by a chi-squared test.

2.5.2 Data mining using the Long Life Family Study (LLFS).

The LLFS was funded by the National Institute on Aging, U.S. National Institutes of Health (grants U01AG023712, U01AG023744, U01AG023746, U01AG023749, and U01AG023755). The data of the LLFS is available using the accession number phs000397.v1.p1. in dbGaP. The study consists of a cohort of 539 families (N=4,953) with siblings, spouses, as well as offspring, who were recruited from Denmark and the United States. The mean age of the first-generation participants (e.g., siblings) was 90 years, whereas the mean age of the remaining participants was 61. The study participants were questioned regarding health, environment, and family history in addition to receiving biomedical testing. All study participants were assayed for 2.5 million

SNPs The SNP LCAD K333Q (rs2286963) was analyzed by Dr. Jatinder Singh for association with measures of lung function, including: FEV1 (the volume of air expelled in the first second), FEV6 (the volume of air expelled in 6 seconds), FEV1/FEV6, LungD (lung disease), COPD (Chronic Obstructive Pulmonary disease), Asthma, and Bronchitis. The analysis was simultaneously adjusted for age, sex, field center, and smoking status (yes or no). Additionally, several markers of immune system function were examined for association with the SNP K333Q genotypes, including: IL6 (Interleukin-6), WBC (white blood cell count), and CRP (C-reactive protein). The replication cohort is Health Aging and Body Composition Study (Health ABC). The Health ABC study was partially funded by the Intra-mural Research Program of the National Institute on Aging (grants AE-2-1024, N01-AG-6-2101, N01-AG-6-2103, and N01-AG-6-2106).

2.5.3 **Antigen-genotype correlation in primary human ATII cells.**

Lysates of primary ATII cells isolated from the same lungs genotyped for K333Q as described above were obtained from Dr. Beata Kosmider and immunoblotted for LCAD. In total, six samples were obtained that were homozygous for the minor Q allele at residue 333 and six samples were obtained that were homozygous for the major K allele. Five µg of total protein of each sample were resolved by SDS-Page (Bio-Rad TGX), transferred to nitrocellulose, and subjected to immunoblotting for LCAD and VLCAD as described above. Additionally, the membrane was stripped and probed with anti-ACAD9 antibody (gift of Dr. Jerry Vockley, 1:2,500). Finally the membrane was stripped and subsequently immunoblotted with anti-acetyllysine antibody as described above. The program Image J was used to perform densitometry. Statistical significance was calculated by a one-tailed Student's t-Test of two samples of unequal variance.

2.6 EVALUATION OF IMMUNE-RELATED PARAMETERS IN LCAD KNOCKOUT MOUSE LUNG

To determine whether loss of LCAD in the lung exacerbates or protects against lung injury, LCAD knockout mice (N=4) and wild type (N=5) were infected with 100 plaque-forming units (PFU) of influenza virus in 50 ul of sterile PBS by oropharyngeal aspiration by Dr. Eric Goetzman and Dr. Chikara Otsubo (University of Pittsburgh). The influenza A/PR/8/34 (H1N1) virus, propagated in chicken eggs, was obtained from Dr. John Alcorn (Children's Hospital of Pittsburgh). Seven days post-infection the mice were sacrificed and lung tissue was harvested, fixed, and stained by Dr. Goetzman and Dr. Otsubo for histology as scored by Dr. Alcorn. Statistical significance was calculated by a one-tailed Student's t-Test of two samples of unequal variance.

Further, surfactant protein-A (SP-A) antigen concentration was examined in mouse lung tissue and bronchial alveolar lavage fluid (BALF). Lung tissue was collected from LCAD KO mice and strain-matched wild type controls. Lysates were prepared by homogenizing the lung tissue using a bullet blender (Next Advance Bullet Blender ™ 24) in RIPA buffer (Pierce) with protease inhibitors (Roche cOmplete, Mini) and phosphatase inhibitors (Boston BioProducts Phosphatase Inhibitors Cocktail-II) as described above. Western blotting for SP-A was conducted as described above for other antigens, using 50 μg of total lysate. BALF samples were blotted per unit of volume, with 40 μL loaded per lane. The primary antibody was anti-SP-A (SFTPA1) (Proteintech, 1:300) and the secondary was chicken anti-rabbit IgG-HRP (Santa Cruz Biotechnology, 1:600). The program Image J was used to perform densitometry. Statistical significance was calculated by a one-tailed Student's t-Test of two samples of unequal variance.

3.0 RESULTS

3.1 HUMAN LCAD VERSUS MOUSE LCAD

Based on known disparities between human and mouse LCAD expression (high in mouse heart/muscle, absent in human heart/muscle), combined with the lack of bona-fide LCAD-deficient patients, LCAD has been suggested to play little role in human FAO, or possibly to catalyze non-FAO functions in the human. Here, I have conducted an objective comparison of the human and mouse LCAD enzymes. The results of this comparison are expected to provide understanding into the biochemical role of human LCAD, the usefulness of the LCAD knockout animal model for investigating LCAD-related pathologies, and clues regarding the potential disease phenotype of an LCAD-deficient human.

3.1.1 Mouse LCAD is more active than human LCAD.

If human LCAD fulfills a different biochemical role than the mouse enzyme, then its enzymatic properties may be altered. To address this question I utilized the simplest system possible: purified recombinant proteins. This system allowed for head-to-head comparison of the biochemical properties of mouse and human LCAD.

First, the steady-state activities of mLCAD and hLCAD Wt recombinant proteins were measured using a range of acyl-CoA substrates from 12 carbons (C_{12}-CoA) to 18 carbons (C_{18}-

CoA). A monounsaturated C18 substrate was also included ($C_{18:1}$-CoA), since this is a particularly abundant fatty acid *in vivo*, and to examine any differences in response to unsaturated fatty acids (Cox K.B., et al. 2001). Each enzyme was assayed with each substrate in at least triplicate using the ETF fluorescence reduction assay under anaerobic conditions as described above.

The steady-state specific activity with saturating substrate concentrations was significantly higher in mLCAD across all substrates tested (Figure 8). Thus, this data suggests that the two enzymes are not biochemically equivalent; mLCAD is more active.

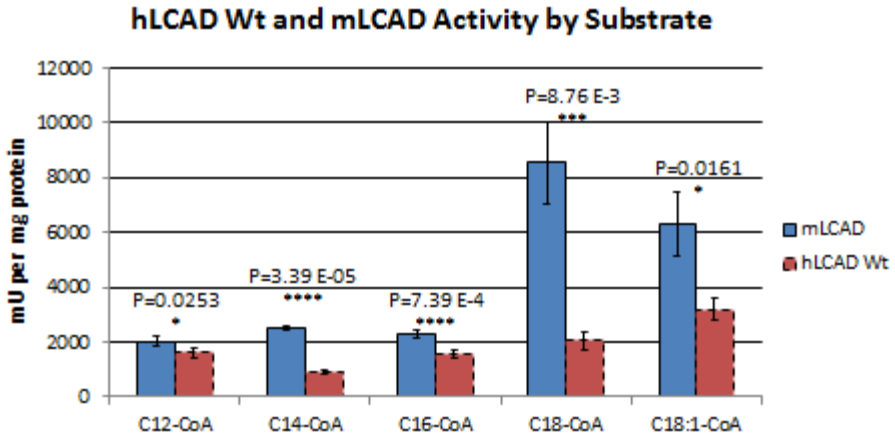

Figure 8: Enzyme Activity Assay of hLCAD Wild Type and mLCAD with Substrates C_{12}-CoA, C_{14}-CoA, C_{16}-CoA, C_{18}-CoA, and $C_{18:1}$-CoA

3.1.2 Enzyme kinetics assays of human and mouse LCAD.

The minimal difference in enzymatic activity between mLCAD and hLCAD when assayed with saturating concentrations of C_{12}-CoA suggested that the two enzymes may be functionally equivalent with this substrate. C_{12}-CoA is a key chain length of substrate because it bridges the

gap between the activity profiles of VLCAD (C_{12} to C_{20}) and MCAD (C_4 to C_{16}), both of which have detectable but low activity against C_{12}-CoA (Souri M., et al. 1998) (Finocchiaro G., et al. 1987) (Swigoňová Z., et al. 2009). To further study species differences with regard to this substrate, a kinetics assay was performed by assaying enzymatic activity of recombinant enzymes over a wide and decreasing concentration range of C_{12}-CoA and kinetic constants were calculated. Activity in the kinetics assay was expressed in units of µM of ETF reduced per minute. The Vmax of hLCAD Wt with the substrate C_{12}-CoA was 1.3 µM/min (Figure 9). The Km, which represents the concentration of substrate at which the activity is half maximal, was 6.9 µM, which is considerably higher than other ACAD enzymes when assayed with optimal or near-optimal substrates (Le W., et al. 2000). In keeping with the steady-state assays, which essentially represent Vmax, mLCAD had a very similar calculated Vmax to hLCAD with C_{12}-CoA (1.2 µM/min), but the Km was considerably lower (2.4 µM) (Figure 9), indicating that mLCAD would be predicted to be more efficient at physiological substrate concentrations. Indeed, the calculated catalytic efficiency of mLCAD was five times higher than hLCAD Wt (3.4 $\mu M^{-1}sec^{-1}$ versus 0.7 $\mu M^{-1}sec^{-1}$) (Figure 9).

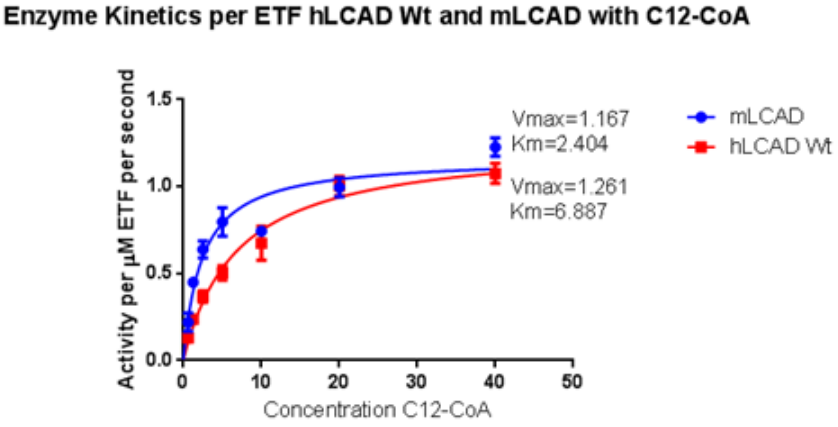

Figure 9: Enzyme Kinetics Assay of hLCAD Wild Type and mLCAD with C_{12}-CoA

3.1.3 **Investigating mechanisms behind the lower catalytic efficiency of hLCAD.**

Given the difference in K_m for C_{12}-CoA between mLCAD and hLCAD, I hypothesized that mLCAD may have a higher affinity than hLCAD Wt for acyl-CoA substrates. To compare the ability of the enzymes to bind substrates, an anaerobic substrate titration experiment was performed. Under these conditions, electrons are removed from the acyl-CoA substrate and passed to the FAD rings, and as it becomes reduced, the FAD loses its characteristic absorbance near 443 nm. At the same time, a broad band forms at around 570 nm, which represents the charge-transfer complex, in which the reduced LCAD enzyme, still bound to enoyl-CoA product, awaits resolution of the complex via transfer of electrons to ETF (Figures 10 and 11). The focus of this assay is the reduction of FAD represented by the decrease in the absorbance of FAD near 443nm normalized by the absorbance at 800 nm. Surprisingly, when the FAD absorbance peak values from Figures 10 and 11 were plotted against substrate concentration (Figure 12), it was clear that the two enzymes had similar abilities to reduce FAD and similar affinities for the C_{12}-CoA substrate. Thus, differences in substrate binding and reducing the FAD do not explain the lower Km and higher catalytic efficiency of mLCAD toward C_{12}-CoA.

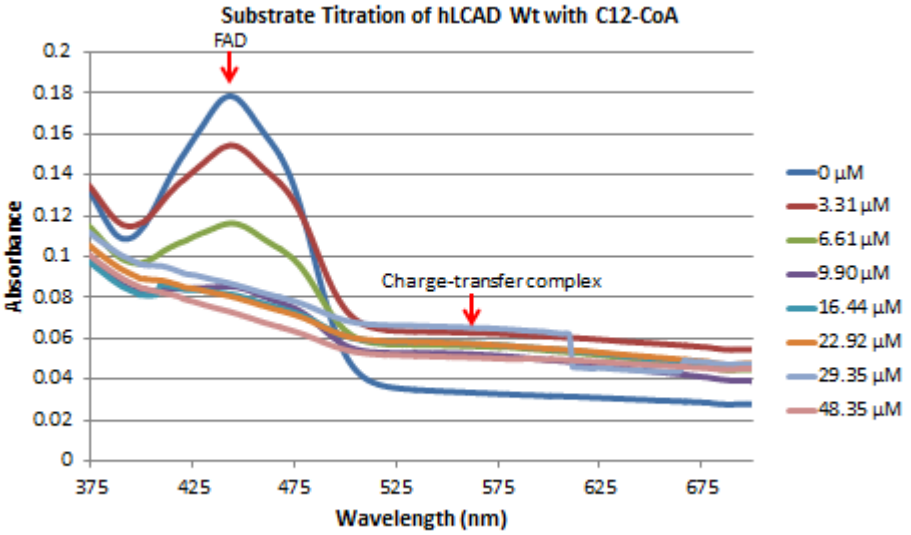

Figure 10: Spectra of Substrate Titration of Human LCAD Wild Type with 0 µM to 48.35 µM of C_{12}-CoA

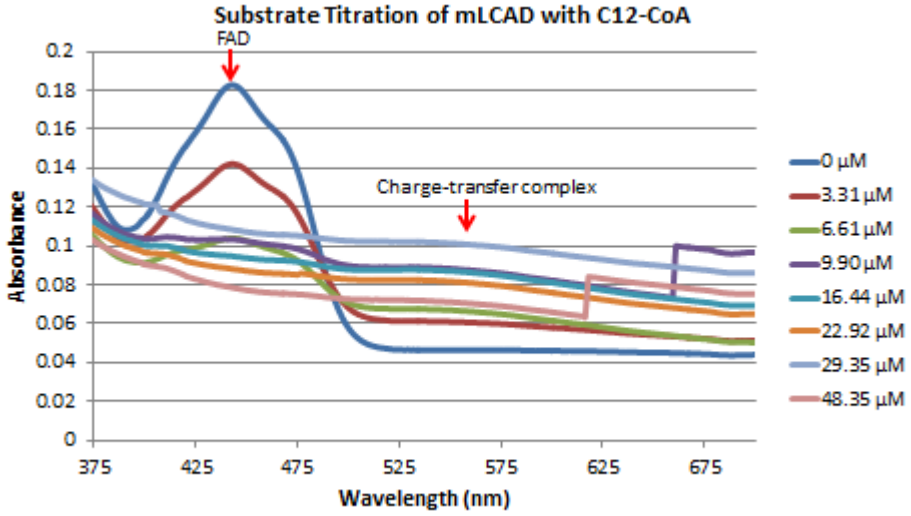

Figure 11: Spectra of Substrate Titration of Mouse LCAD with 0 µM to 48.35 µM of C_{12}-CoA

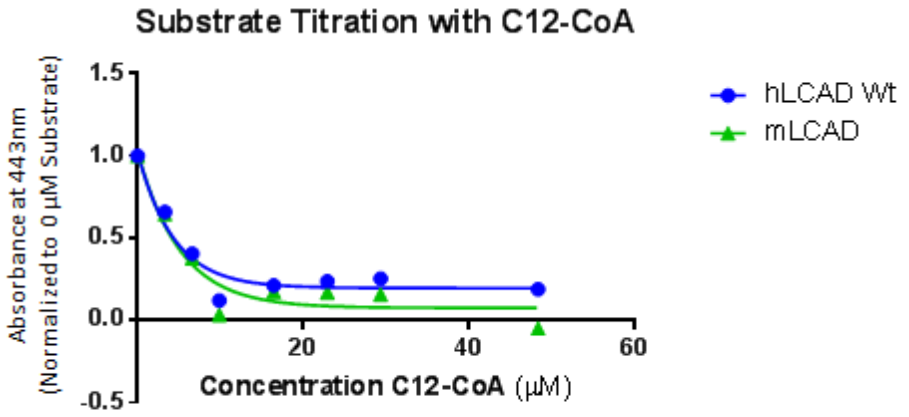

Figure 12: Substrate Titration of Human LCAD Wild Type and Mouse LCAD with 0 µM to 48.35 µM of C_{12}-CoA

3.1.4 Stability of hLCAD and mLCAD.

Another mechanism explored to explain the lower catalytic efficiency and enzymatic activity of hLCAD was protein stability. The lower stability of hLCAD could explain lower function in the activity assays. In preliminary experiments it was noted that the absorbance spectra of recombinant hLCAD changed with extended incubations at 37 °C, particularly with an increase in absorbance at 345nm from an absorbance of approximately 0.05 at 0 hours for recombinant hLCAD Wt enzyme to approximately 0.15 at 48 hours and an absorbance of approximately 0.05 at 0 hours for recombinant hLCAD K333Q enzyme to approximately 0.35 a t 12 hours, suggesting precipitation (Figure 13) (Figure 14).

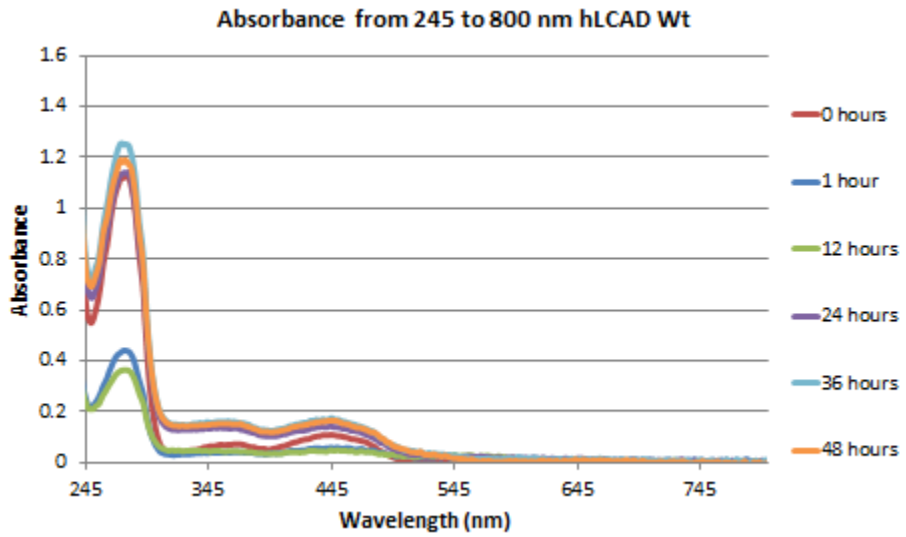

Figure 13: Spectra of hLCAD Wt Incubated at 37°C for 48 Hours

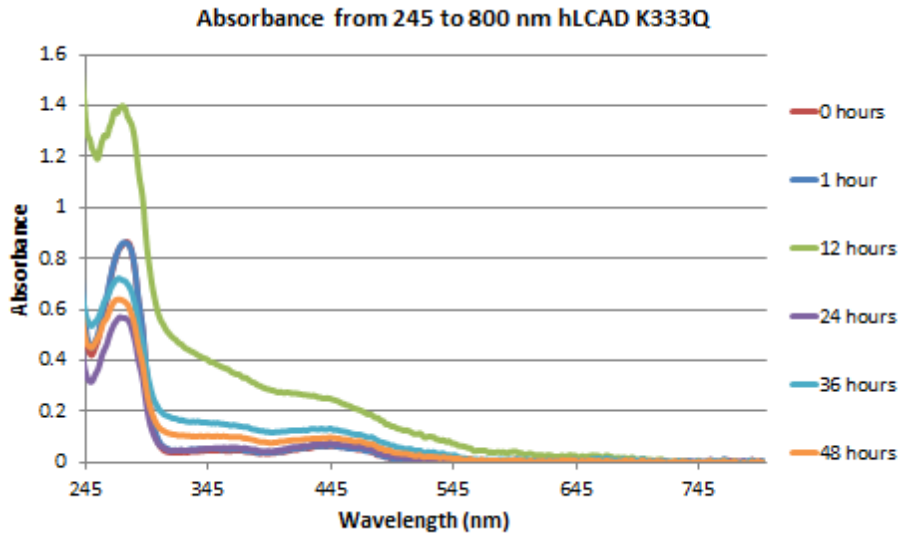

Figure 14: Spectra of hLCAD K333Q Incubated at 37°C for 48 Hours

Therefore, a simple stability assay was designed in which hLCAD and mLCAD were incubated at 0 °C, room temperature, 37 °C, and 55 °C for increasing time periods. At each time point, the proteins were centrifuged to remove precipitated protein and subjected to absorbance scanning. The resulting absorbance scans did not show the abnormal increase in absorbance near

345 nm indicating the that precipitated proteins were successfully removed (see Appendix A). The A_{280} peaks from these scans, chosen to represent the total soluble LCAD protein remaining at each time point, were normalized to absorbance at 0 hours and plotted against time of incubation (Figures 15 and 16). In these latter plots, it is clear that some hLCAD protein is lost from solution after an overnight incubation at 37°C while this is not seen for mLCAD. In contrast, when exposed to the severe temperature of 55°C, both proteins quickly precipitate, and to similar degrees (Figure 17). Thus, hLCAD seems to be modestly less stable than mLCAD, but this is apparent only after extensive incubation (overnight) at 37°C, and therefore does not likely explain the reduced catalytic efficiency in the kinetics assays, which involve only short-term incubations of the proteins at 32°C.

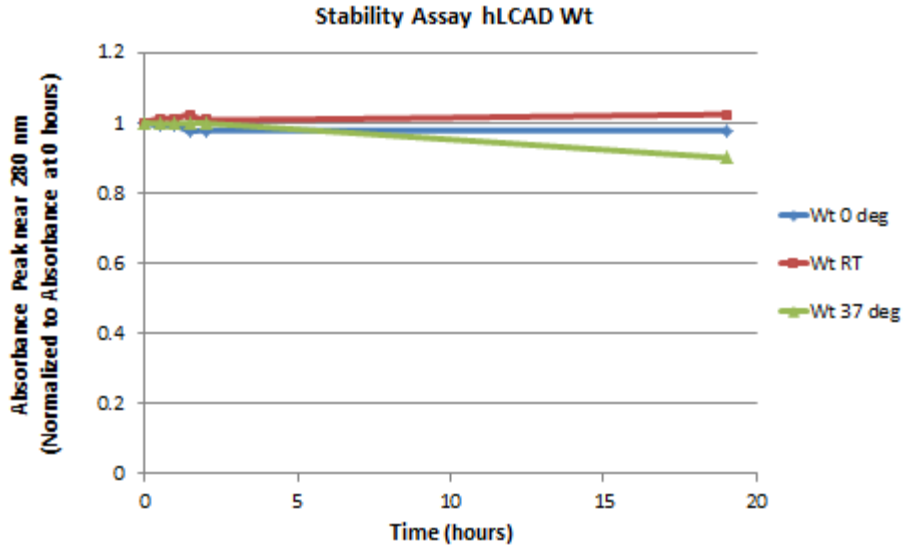

Figure 15: Stability Assay of hLCAD Wt at 0°C, Room Temperature, and 37°C for 0 Hours, 1 Hour, 1.5 Hours, 2 Hours, and 19 Hours Normalized to 0 Hours

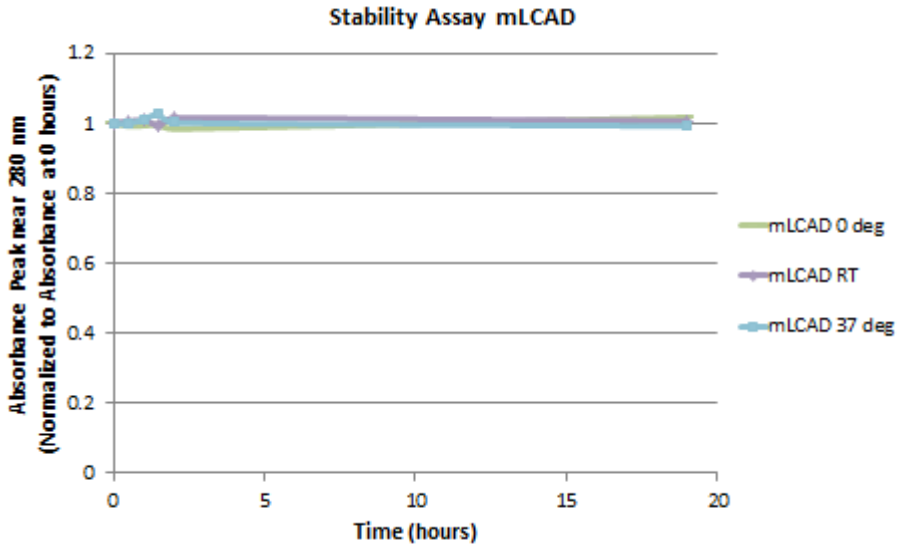

Figure 16: Stability Assay of mLCAD at 0°C, Room Temperature, and 37°C for 0 Hours, 0.5 Hours, 1 Hour, 1.5 Hours, 2 Hours, and 19 Hours Normalized to 0 Hours

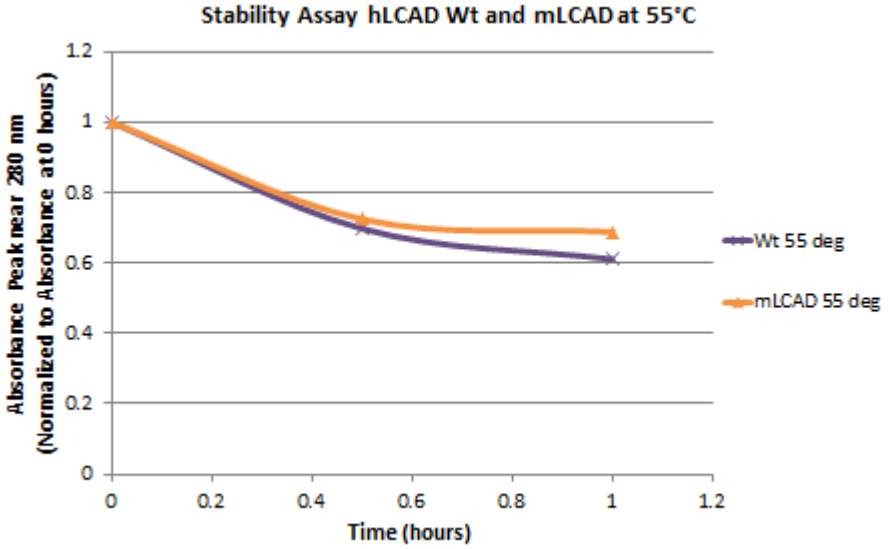

Figure 17: Stability Assay of hLCAD Wt and mLCAD at 55°C for 0 Hours, 0.5 Hours, and 1 Hour Normalized to 0 Hours

3.1.5 Structural differences between mouse and human LCAD.

Finally, the primary amino acid sequences and the three-dimentional crystal structure of hLCAD solved by collaborator Dr. Jung-Ja Kim (unpublished), were analyzed for clues regarding the enhanced biochemical function of mLCAD compared to hLCAD. Mouse LCAD and human LCAD are 87% identical and 93% similar in amino acid sequence (Figure 18) (blast.ncbi.nlm.nih.gov/Blast.cgi). Analysis of the crystal structure of human LCAD with the guidance of Dr. Al-Walid Mohsen bound with C_{12}-CoA revealed that fourteen amino acids were within approximately 3 Å of the C_{12}-CoA substrate, indicating a potential role in binding. One of the substrate-binding amino acids was found to be valine in human LCAD and a leucine in mouse LCAD (Figure 18). Forty-three amino acid residues were found to be within about 3 Å of the FAD cofactor, indicating a potential role for binding, and 40 out of 43 of these amino acid residues are identical between mouse and human LCAD (Figure 18). The three remaining FAD binding residues that were not identical between mLCAD and hLCAD were residues 205, 253, and 327. Two of theses—residues 205 and 253—are conservative substitutions (threonine to serine and isoleucine to leucine) while residue 327 is a methionine in the mouse sequence and leucine in the human sequence. This latter substitution, while not as conservative as the other two, was not predicted to be deleterious when analyzed by the prediction software SIFT. SIFT is a computational algorithm that uses information on the degree of conservation of amino acids in related sequences as well as the properties of amino acids, to assess whether an amino acid change has detrimental effects on enzyme or protein function (SIFT, 2015). Finally, the catalytic base and lysine 333 are conserved between mouse and human LCAD indicating importance of these sites as they remain conserved across species (Figure 18). Therefore, the analysis of the two LCAD sequences did not reveal any amino acid differences to suggest that the human

enzyme has a different function than the mouse enzyme. However, the differences in the amino acid sequence may contribute toward the higher enzymatic activity and catalytic efficiency of mouse LCAD.

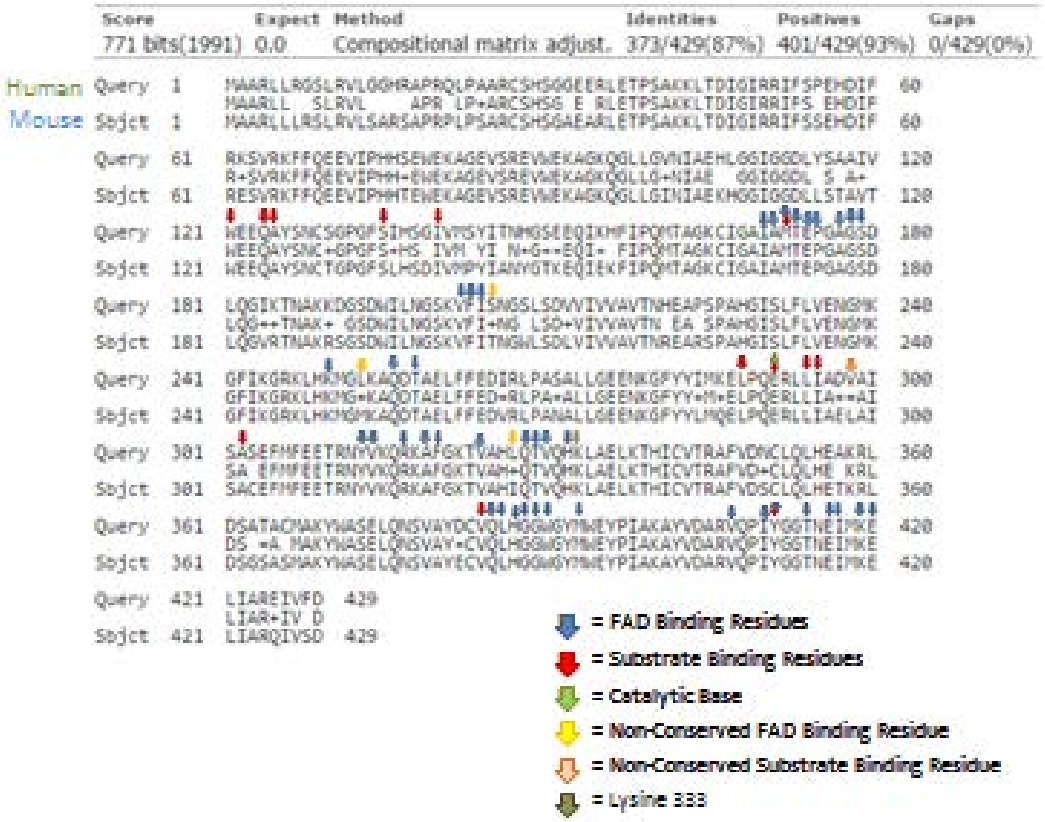

Figure 18: Amino Acid Alignment of Mouse and Human LCAD

3.1.6 **Differences in LCAD expression between mice and humans.**

LCAD is not appreciably expressed in human muscle or heart tissue in which FAO is an important source of energy (He M., et al. 2007). On the other hand, hLCAD is expressed in ATII cells in the lung (Goetzman E.S., et al. 2014). LCAD has also been implicated in the pathogenesis of human prostate and breast cancers (Xie, B.-X., et al. 2011) (Hill, VK, et al., 2011). Therefore, I hypothesized that LCAD may have a role in human tissues not typically

reliant on FAO, particularly in secretory epithelial cells such as ATII cells or the epithelia of the breast and prostate. To examine the possible role of LCAD in these secretory tissues, the expression of LCAD was experimentally examined in human tissue lysates. The expression of VLCAD was examined concurrently given that the substrate specificity of VLCAD overlaps with LCAD, so possible compensation for a deficiency of LCAD could be determined and to gain insight into the relative role of these two long-chain ACAD enzymes. Equal amounts of total protein lysates from human breast, kidney, liver, lung, pancreas, prostate, and thyroid tissue (G Biosciences) as well as mouse kidney, liver, lung, and pancreas tissue were Western-blotted with anti-LCAD and anti-VLCAD antibodies, with Ponceau staining as a loading control (Figure 19). Contrary to my hypothesis, hLCAD was most abundantly expressed in the liver, followed by kidney, lung, and pancreas. Human breast, prostate, and thyroid showed little or no detectable LCAD protein. VLCAD was similarly highly expressed in human liver, kidney, and pancreas with little or no antigen in breast, prostate, or thyroid. LCAD appeared to dominate over VLCAD in human lung tissue, as only trace amounts of the short isoform of VLCAD were detectable in human lung lysate, and no visible VLCAD antigen in mouse lung tissues (Figure 19). Also, there seems to be more VLCAD antigen in human pancreas lysate than mouse lysate. Additionally, there seems to be more LCAD in the liver than in the kidney in human tissue lysates, but similar amounts of LCAD antigen in mouse kidney and liver tissue lysates (Figure 19A).

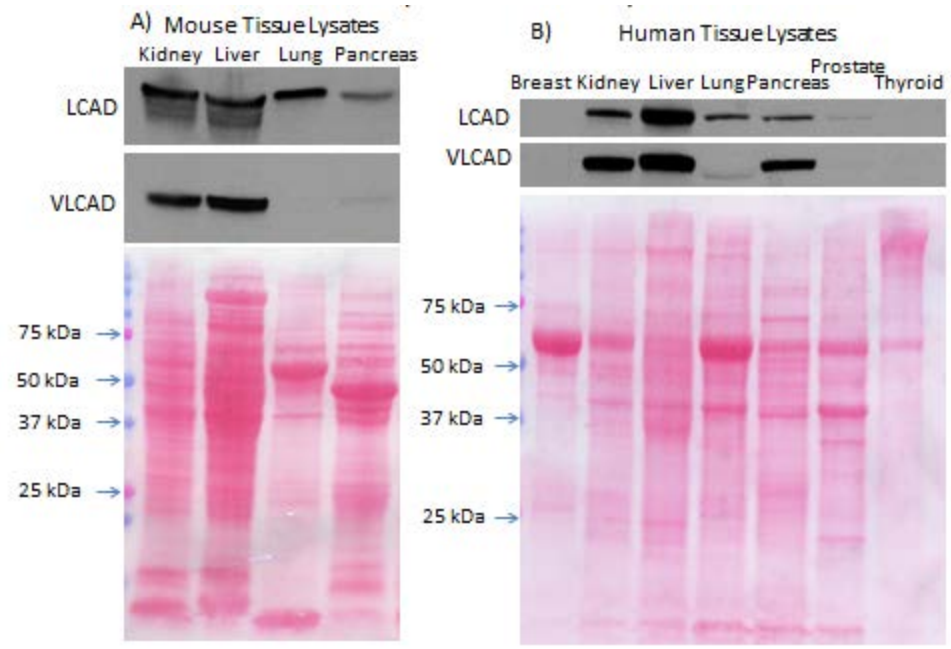

Figure 19: Western Blots of LCAD and VLCAD Antibodies of 50 µg of A) Mouse and B) Human Tissue Lysates

3.1.7 Quantification of LCAD and VLCAD in human and mouse hepatocytes.

As Figure 19 shows, mice and humans both appeared to co-express LCAD and VLCAD in the liver. This may be of clinical significance as it indicates that hLCAD may be able to compensate for the loss of VLCAD in VLCAD-deficient patients. To further investigate this co-expression, an experiment was designed to quantify the amount of LCAD and VLCAD antigen in the primary hepatocytes isolated from humans and mice. Hepatocytes were examined as they account for the largest percentage of cell population of the liver, and are an important site of fatty acid metabolism (Wang Y. and Hay D.C. 2016) (Fox I.J., et al. 1998). A standard curve of known amounts of recombinant LCAD and VLCAD from 20 ng to 80 ng were immunoblotted alongside 25 µg of human and mouse hepatocyte lysates (Figure 20). LCAD antigen in primary human hepatocyte lysates and more LCAD antigen than VLCAD antigen.

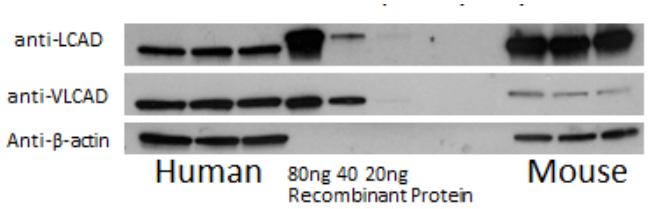

Figure 20: Western Blot of LCAD and VLCAD in 25 µg of Human and Mouse Hepatocyte Lysates

The program Image J was used to quantify the standard curve of each recombinant protein with densitometry and determine the unknown quantity of LCAD and VLCAD in the hepatocyte lysates (Figure 21). Human hepatocyte lysates had about half as much LCAD antigen per µg of total protein than mouse hepatocytes (1.9ng of LCAD per µg versus 3.5 ng per µg), while VLCAD was four times more abundant (3.1 ng per µg for human versus 0.8 ng per µg for mouse).

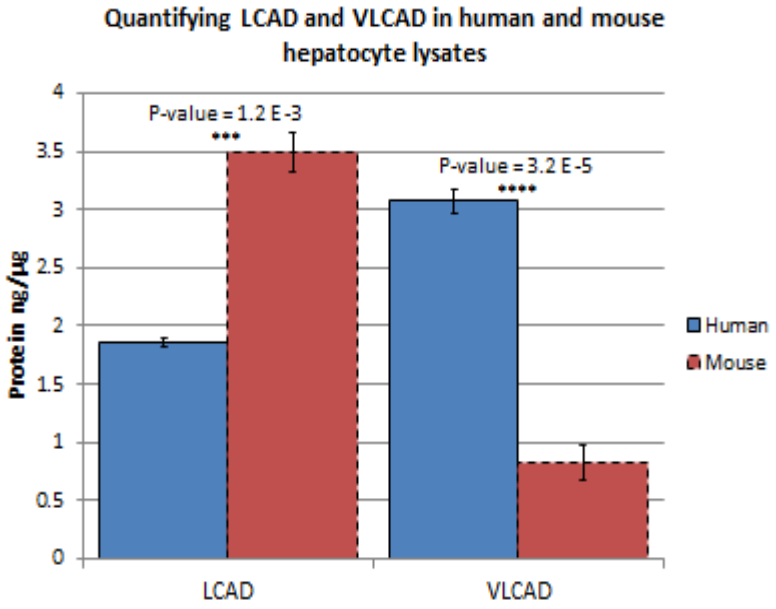

Figure 21: Quantification of ng of LCAD and VLCAD per µg of Hepatocyte Lysate

3.1.8 **Conclusions.**

The amino acid sequences of mouse and human LCAD are largely conserved, and ability of human and mouse LCAD to bind a substrate and reduce FAD are similar. However, the phenotype of LCAD knockout mice resembles the phenotype of human VLCADD (Chegary M., et al. 2009) (Cox K.B., et al. 2001) (Kurtz D.M., et al. 1998). Furthermore, some investigators have suggested that mLCAD and hLCAD are not functional equivalents (Maher A.C., et al. 2010). My results indicated that the enzyme activity of mLCAD is higher than hLCAD Wt activity for all substrates tested (Figure 8), suggesting that the two enzymes are not functionally equivalent. This was further supported by kinetic assays that demonstrated that mLCAD has considerably higher catalytic efficiency than hLCAD Wt (Figure 9). Furthermore, mLCAD was somewhat more stable than hLCAD Wt at 37 ºC (Figure 15) (Figure 16). Finally, the tissue expression of LCAD and VLCAD were shown to be different between human and mouse primary hepatocytes. Surprisingly, hLCAD is more abundant in human hepatocytes that previously suggested in the literature (half as abundant as in mouse hepatocytes). A much larger differential between species was noted for VLCAD, which appears to be weakly expressed in the mouse. This may explain why VLCAD knockout mice have a mild phenotype. Human hepatocytes rely somewhat more on VLCAD than LCAD, whereas mouse hepatocytes rely very heavily on LCAD (Figure 20) (Figure 21). When taken together, these studies suggest that LCAD may not serve the same function in humans as it does in mice, Further, it suggests that the LCAD/VLCAD knockout models may not be representative of their respective human phenotypes.

3.2 HUMAN LCAD WILD TYPE AND THE CONSEQUENCES OF HUMAN LCAD K333Q

While there have been no identified patients in the literature, our laboratory has previously described two cases of SUID with no measurable LCAD antigen in the lung. Both were homozygous for a common polymorphism, K333Q. Although the amino acid sequence alignment shows that the lysine in SNP K333Q is not an FAD binding residue, it is adjacent to the FAD binding residue, Histidine 332 (Figure 18). The crystal structure reveals that lysine 333 (K333) is about 6.06 Å away from the FAD in the crystal structure. Therefore, a change to glutamine at site 333 may have indirect consequences to FAD binding and/or enzymatic activity in human LCAD. Additionally, lysine 333 is conserved between mouse and human LCAD (Figure 18). It was therefore hypothesized that this polymorphism may be detrimental to LCAD function. Furthermore, because the lung represents a tissue where hLCAD is dominant with little VLCAD co-expression, it was hypothesized that K333Q may be a risk factor for human lung disease. These hypotheses were investigated through examination of the crystal structure, biochemical characterization of recombinant LCAD K333Q, and genotyping of disease populations for the SNP K333Q.

3.2.1 Human LCAD crystal structure.

The crystal structure of human wild-type LCAD containing C_{12}-CoA in the substrate-binding pocket was obtained from Dr. Jung-Ja Kim (unpublished) (Figure 22).

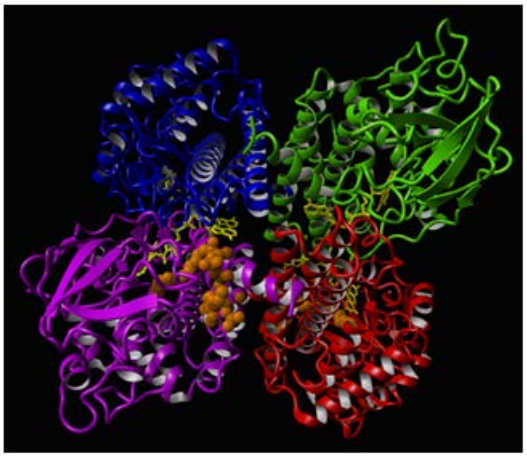

Figure 22: Crystal Structure of Human LCAD Wild Type: Four subunits forming a homotetramer are shown. The yellow ring structure are FAD bound in the active site, and the orange ball strutures are bound substrate

Analysis of the structure reveals that, like other ACADs, LCAD forms a homotetramer with the binding pockets of the active sites toward the center, where the vital FAD and the acyl-CoA substrate are bound. As described previously, analysis of the crystal structure revealed that while each monomer is associated with an FAD cofactor, FAD binding is cooperative, such that each FAD is bound by amino acids from three different subunits of the LCAD homotetramer. Twenty-five amino acids from one subunit have the potential to bind FAD, with further contribution from 16 amino acids on the adjacent subunit and two amino acids (Gln328 and Val330) from a third subunit of the homotetramer. Importantly, the amino acid residue K333 that changed from a lysine to a glutamine in the SNP K333Q is adjacent to histidine 332 that is predicted to bind FAD. This analysis suggests that any alteration at residue K333, i.e., polymorphism K333Q, may have deleterious effects on enzymatic assembly and/or function.

3.2.2 **Enzyme activity assays of human LCAD wild type and K333Q.**

Given the proximity of residue K333 to the active site of human LCAD, I hypothesized that the polymorphism K333Q would indeed inhibit the enzymatic function of hLCAD. This hypothesis was examined experimentally using the steady-state ETF fluorescence reduction assay with recombinant enzymes. The sequence of the plasmid for the recombinant enzyme, hLCAD K333Q, changes the wild type lysine to a glutamine at site 333 for all monomers of the purified protein. Compared to recombinant hLCAD, recombinant hLCAD K333Q demonstrated significantly reduced enzymatic activity for multiple acyl-CoA substrates including C_{12}-CoA, C_{14}-CoA, C_{16}-CoA, C_{18}-CoA, and $C_{18:1}$-CoA (Figure 23).

.

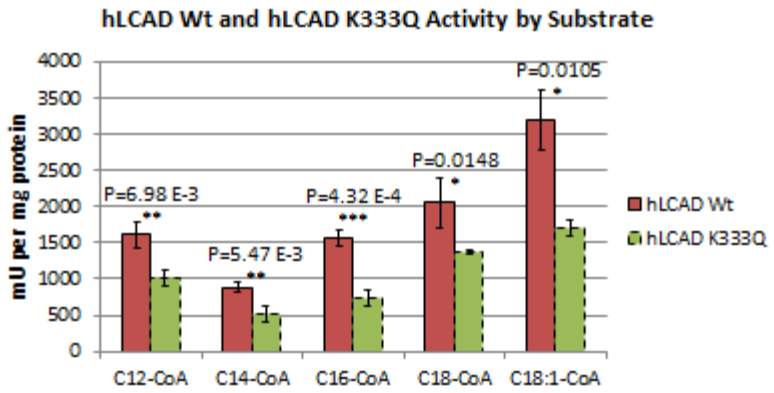

Figure 23: Enzyme Activity Assay of hLCAD Wild Type and hLCAD K333Q with C_{12}-CoA, C_{14}-CoA, C_{16}-CoA, C_{18}-CoA, and $C_{18:1}$-CoA

3.2.3 Enzyme kinetics assays of recombinant hLCAD and hLCAD K333Q.

The data in Figure 24 indicated that the polymorphic LCAD enzyme is less active than wildtype hLCAD when assayed with saturating substrate concentrations. To further probe this difference, kinetic assays were performed using a range of C12-CoA (near 0.6 µM to near 40 µM). To account for any differences in FAD content, the activity data for the kinetics assay was normalized to the FAD absorbance (443 nm) rather than to protein concentration. The V_{max} of wild-type hLCAD was 1.3 µM/min and the K_m for C_{12}-CoA was 6.9 µM (Figure 24). Surprisingly, hLCAD K333Q showed enhanced activity with lower substrate concentrations, and thus, while the V_{max} was similar to the wild-type enzyme (1.2 µM/min) the K_m was considerably lower (2.2 µM). As a result of the lower K_m, the calculated catalytic efficiency of the K333Q mutant was higher than hLCAD Wt (2.5 $\mu M^{-1}sec^{-1}$ versus 0.7 $\mu M^{-1}sec^{-1}$) (Figure 24). This result indicates that the hLCAD wild type seems to be less efficient at catalyzing the reaction with C_{12}-CoA than hLCAD K333Q.

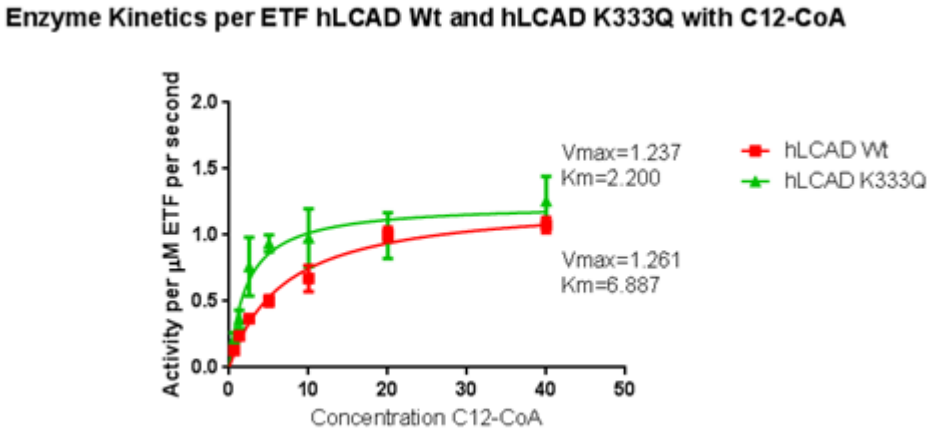

Figure 24: Enzyme Kinetics Assay of hLCAD Wild Type and hLCAD K333Q with C_{12}-CoA

3.2.4 **Substrate titration assays human LCAD wild type and K333Q.**

The reductive half-reaction of LCAD can be assessed by incubating the enzyme under anaerobic conditions with increasing amounts of substrate. Under these conditions, electrons are removed from the acyl-CoA substrate and passed to the FAD rings, and as it becomes reduced, the FAD loses its characteristic absorbance at 443 nm. At the same time, a broad band forms at around 570 nm, which represents the charge-transfer complex, in which the reduced LCAD enzyme, still bound to enoyl-CoA product, awaits resolution of the complex via transfer of electrons to ETF. To determine if K333Q alters the reductive half-reaction, the recombinant enzyme with a change from lysine to glutamine at site 333 for all monomers (hLCAD K333Q) and its wild-type counterpart were titrated with increasing amounts of three different acyl-CoA substrates. An example of the creation of the charge-transfer complex as demonstrated by the increase in absorbance at 570 nm is seen in Figure 25. Figure 25 represents the formation of the charge-transfer complex by showing the increasing absorbance of the peak at 570nm normalized by subtracting the absorbance at 800nm. The focus of this assay is the reduction of FAD represented by the decrease in the absorbance of FAD near 443nm normalized by the absorbance at 800nm. For all three substrates tested, C_{12}-CoA, C_{16}-CoA, and C_{18}-CoA, recombinant hLCAD K333Q did not reduce in absorbance as much as hLCAD Wt enzyme (Figure 10) (Figures 26-33). Therefore, hLCAD K333Q had decreased ability to bind substrates or to reduce the cofactor FAD as compared to hLCAD wild type. One possible interpretation is that the four subunits of LCAD, each of which normally contains an FAD, work cooperatively for maximum abstraction of electrons and formation of the charge-transfer complex. Partial loss of FAD combined with de-stabilization at the monomer-monomer interfaces, caused by K333Q, may block inter-subunit cooperativity and prevent the enzyme FAD from becoming completely reduced.

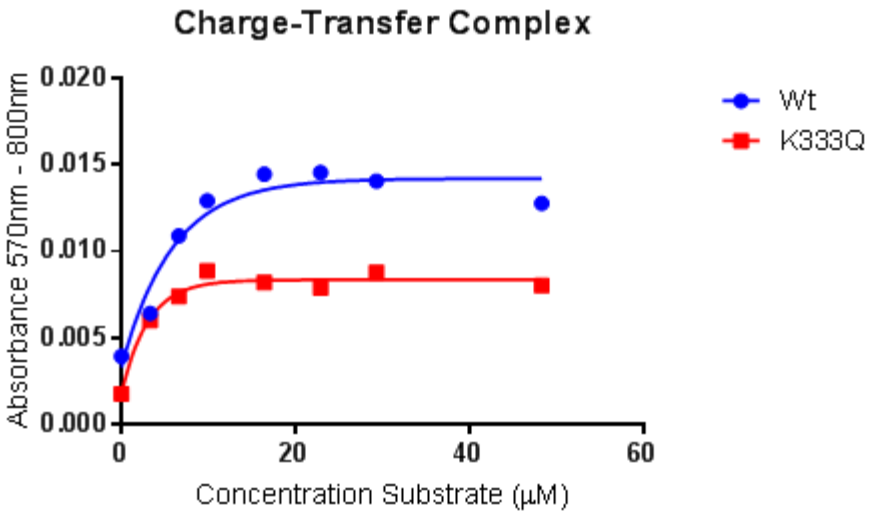

Figure 25: Charge-Transfer Complex Measured by Absorbance of 570nm-800nm of hLCAD K333Q with 0 µM to 48.35 µM of C_{16}-CoA

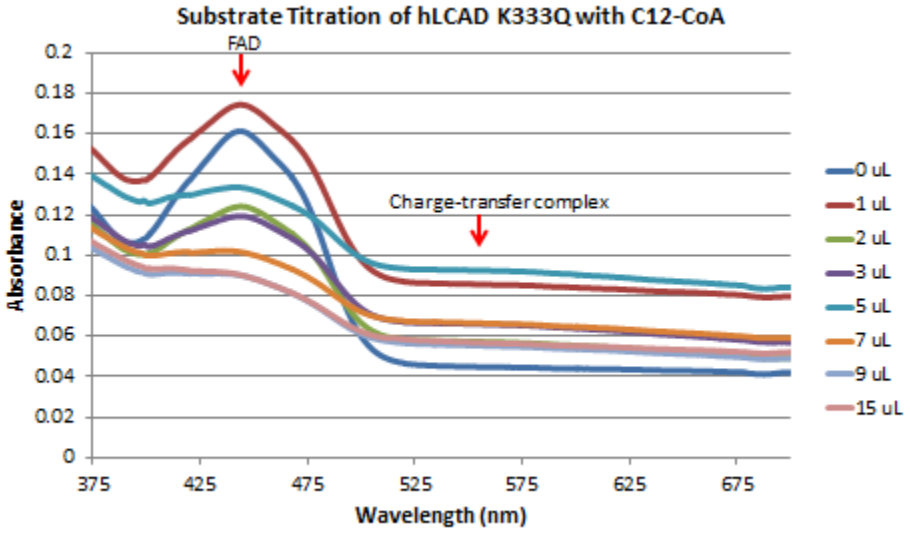

Figure 26: Spectra of Substrate Titration of hLCAD K333Q with 0 µM to 48.35 µM of C_{12}-CoA

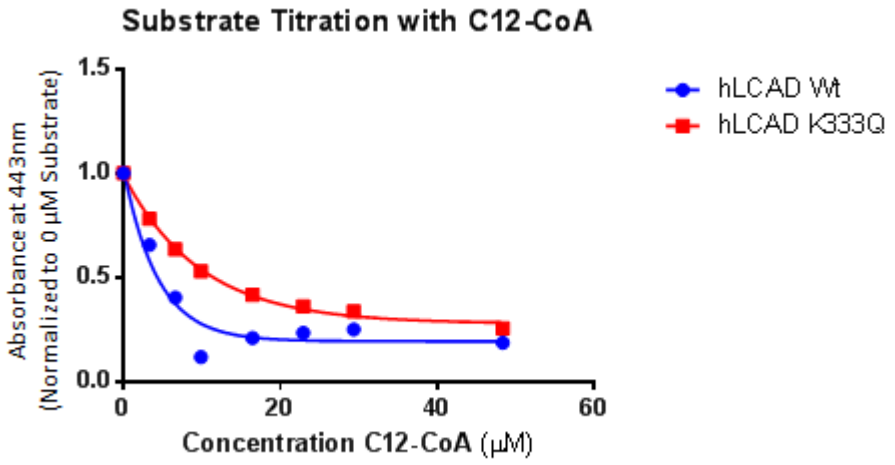

Figure 27: Substrate Titration Assay of hLCAD Wt and hLCAD K333Q with C_{12}-CoA from 0 µM to 48.35 µM

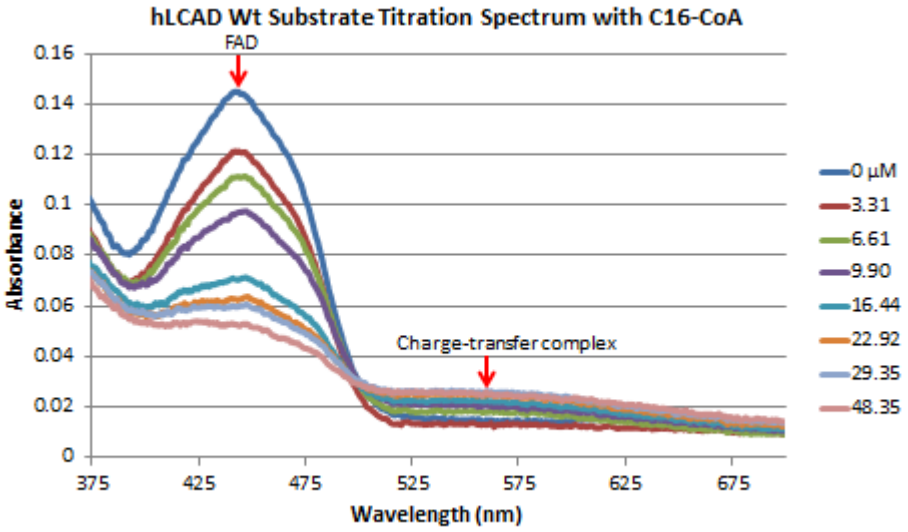

Figure 28: Spectra of Substrate Titration of hLCAD Wt and 0 µM to 48.35 µM of C_{16}-CoA

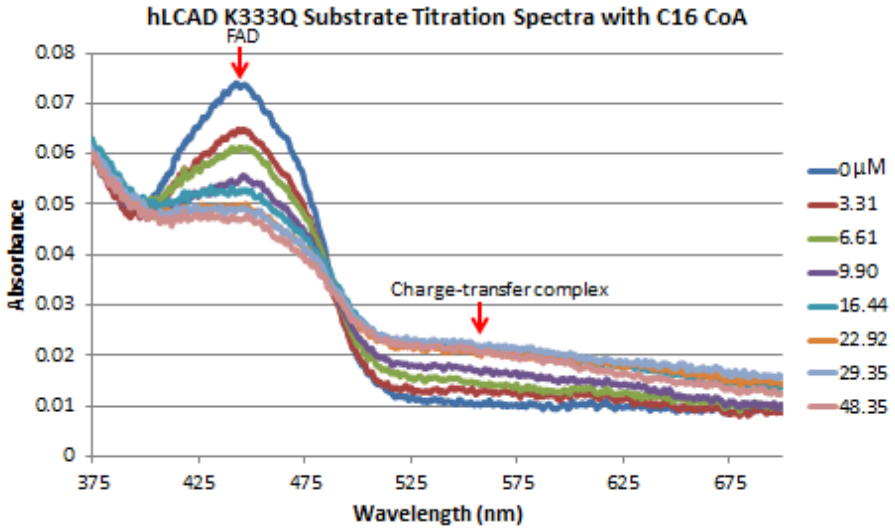

Figure 29: Spectra of Substrate Titration of hLCAD K333Q with 0 µM to 48.35 µM of C_{16}-CoA

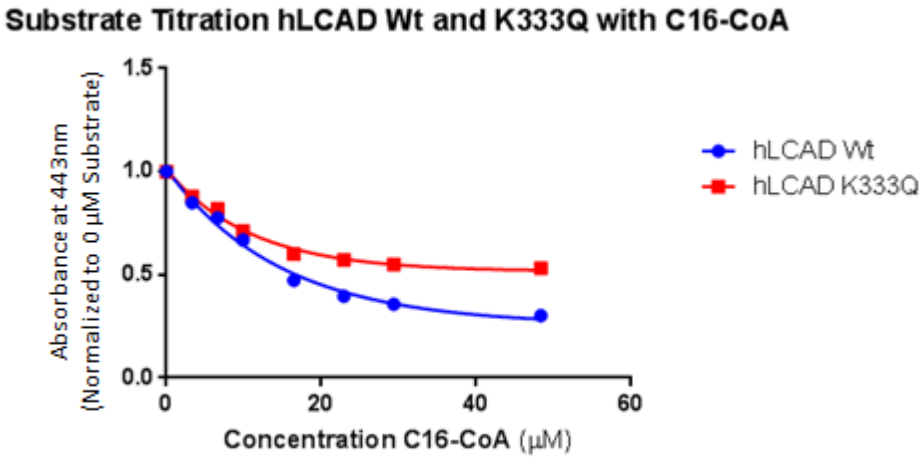

Figure 30: Substrate Titration of hLCAD Wt and hLCAD K333Q with C_{16}-CoA from 0 µM to 48.35 µM

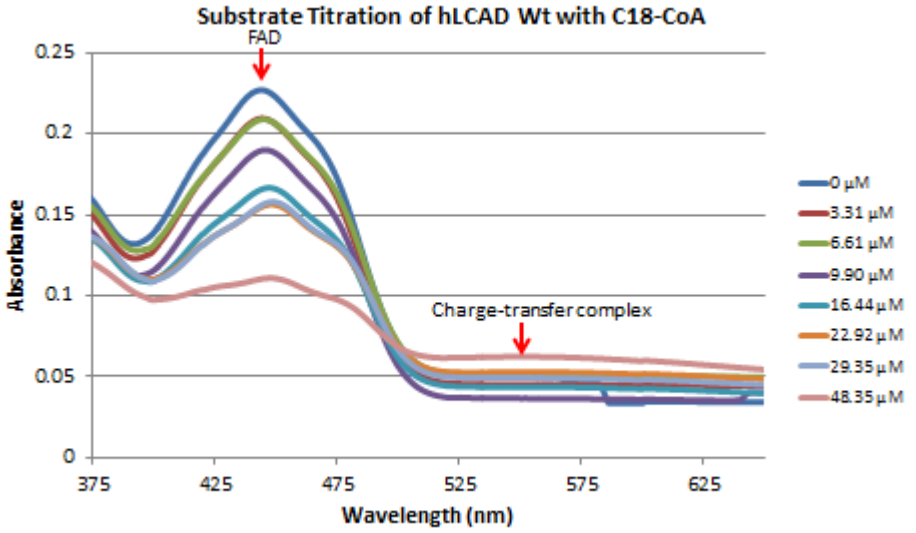

Figure 31: Spectra of Substrate Titration of hLCAD Wt with 0 µM to 48.35 µM of C_{18}-CoA

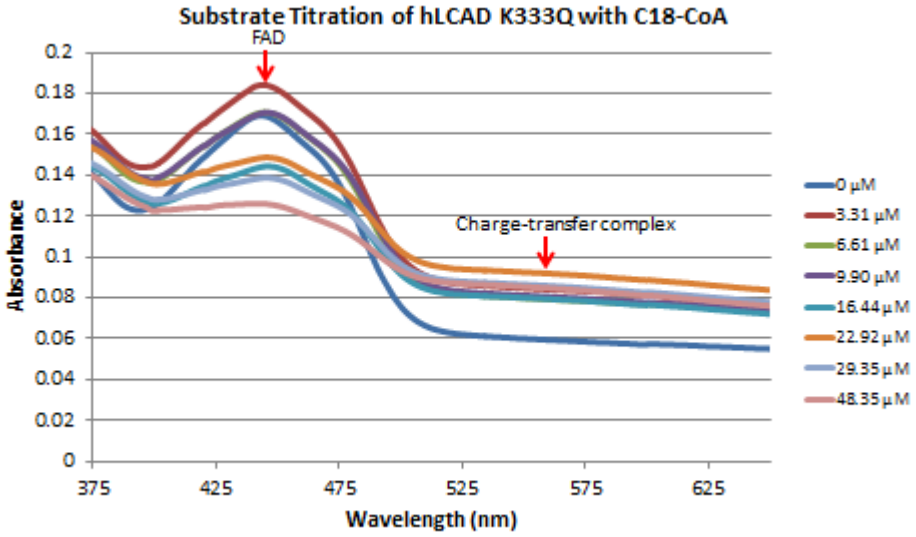

Figure 32: Spectra of Substrate Titration of hLCAD K333Q with 0 µM to 48.35 µM of C_{18}-CoA

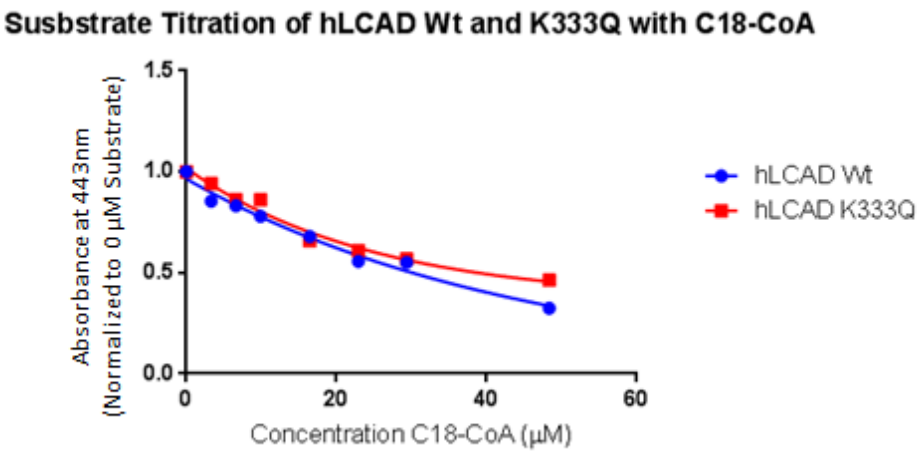

Figure 33: Substrate Titration of hLCAD Wt and hLCAD K333Q with C_{18}-CoA from 0 µM to 48.35 µM

3.2.5 Stability assay of human LCAD wild type and K333Q.

Given the position of K333 at the monomer-monomer interface and its proximity to important FAD-binding residues such as H332, I hypothesized that substitution K333Q may destabilize the LCAD homotetramer. Indeed, the stability assay of recombinant hLCAD wild type and hLCAD K333Q incubated at 0 °C, room temperature, 37 °C, and 55 °C for 19 hours showed that hLCAD Wt seems to be more stable than hLCAD K333Q. At 0 °C and room temperature there was no precipitation in either hLCAD Wt or K333Q after 19 hours of incubation (Figure 15) (Figure 34). However, it was shown that at 37 °C there was precipitation of both hLCAD Wt and K333Q proteins, but the effect was greater for the mutant K333Q. A greater percentage of hLCAD K333Q protein precipitates at 37 °C with the absorbance of the peak near 280 was reduced by approximately 10% after 19 hours and as compared to approximately 30% for hLCAD K333Q (Figure 15) (Figure 34). Additionally, with incubation at 55 °C, both hLCAD Wt and hLCAD K333Q showed rapid precipitation beginning around 0.5 hours of incubation. After 1 hour at 55

°C the absorbance peak near 280 nm was reduced by approximately 30% for hLCAD wild type versus approximately 55% for hLCAD K333Q (Figure 35).

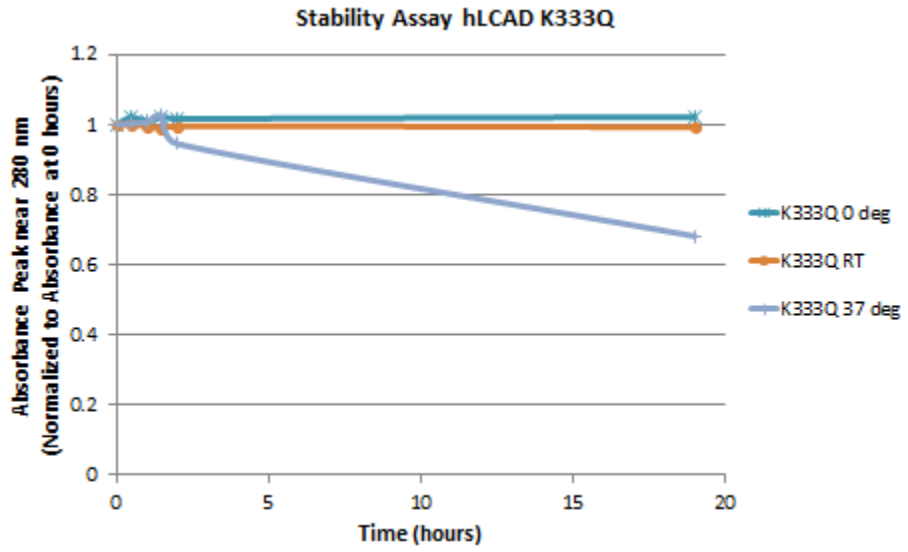

Figure 34: Stability Assay of hLCAD K333Q at 0°C, Room Temperature, and 37°C for 0 Hours, 0.5 Hours, 1 Hour, 1.5 Hours, 2 Hours, and 19 Hours Normalized to 0 Hours

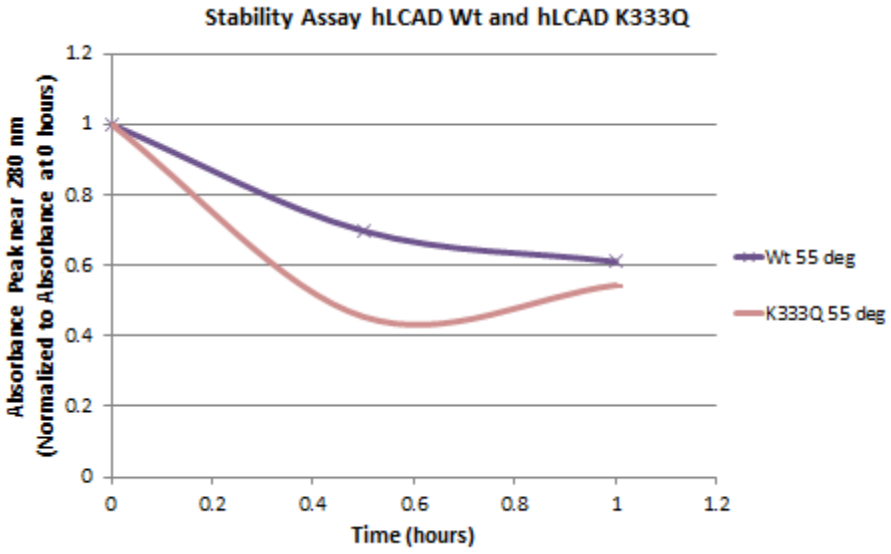

Figure 35: Stability Assay of hLCAD Wt and hLCAD K333Q at 55°C for 0 Hours, 0.5 Hours, and 1 Hour Normalized to 0 Hours

3.2.6 Rescuing loss of FAD with exogenous FAD.

The bound FAD cofactor provides a distinct yellow color to purified recombinant LCAD, which was noticeably paler in for purified hLCAD K333Q as compared to purified recombinant hLCAD Wt. This suggests a lower FAD content in the K333Q mutant protein, which would explain the lower enzymatic activity of hLCAD K333Q and impaired reduction of FAD and formation of the charge-transfer complex. To examine this hypothesis, I performed an experiment to measure the FAD ratio through spectral scans of the recombinant protein. The FAD ratio is calculated as the ratio of FAD as measured by the absorbance near 445 nm by the total protein as measured by the absorbance near 280 nm. An FAD ratio of approximately 8 indicates normal binding of FAD and an FAD ratio above 10 indicates of loss of the FAD cofactor. Lost FAD cofactors can be replaced through incubation of purified LCAD protein with

exogenous FAD (Nagao M. and Tanaka K. 1992). The spectra of recombinant hLCAD Wt and hLCAD K333Q were obtained to calculate the FAD ratios (Figure 36), and indeed, mutant K333Q was associated with a partial loss of FAD from the protein. Then, it was determined if the loss of FAD, as well as the reduced enzymatic activity, could be rescued with incubation of exogenous FAD. Both Wt hLCAD and the mutant K333Q showed significantly improved FAD ratios following incubation with exogenous FAD (Table 1), and in keeping with this, enzymatic activity was also increased for both proteins (Figure 37). The incubation of recombinant hLCAD with exogenous FAD decreased the FAD ratios of hLCAD by reducing the ratios of both hLCAD Wt from 8.16 to 6.64 and hLCAD K333Q from 12.11 to 9.70 (Table 1). Exogenous FAD significantly increased the enzymatic activity of both hLCAD wild type and hLCAD K333Q (Figure 37). However, even after FAD rescue, the enzymatic activity of hLCAD K333Q remained significantly lower than FAD-treated hLCAD Wt ($P = 1.77\ E^{-4}$) (Figure 37).

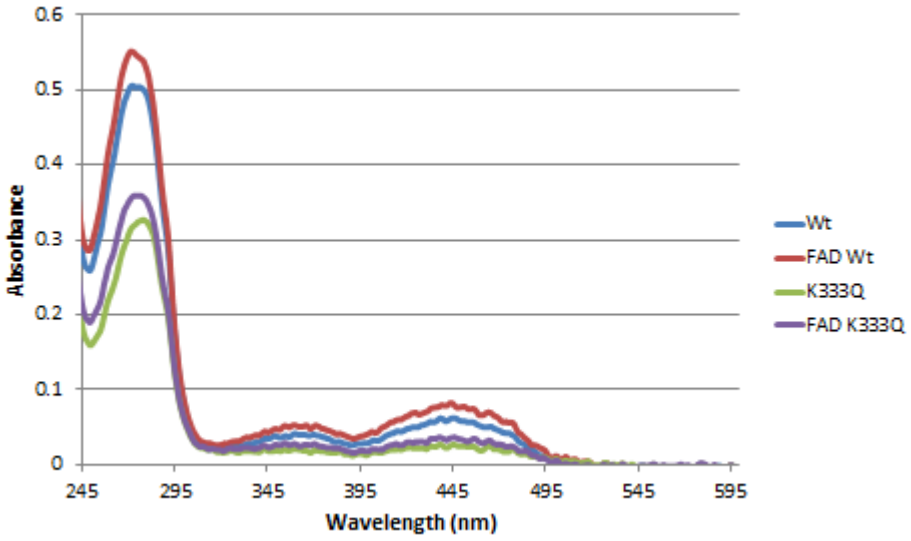

Figure 36: Spectra of hLCAD Wt and hLCAD K333Q Treated and Untreated with Exogenous FAD

Table 1: FAD Ratios of hLCAD Wt and hLCAD K333Q Treated and Untreated with Exogenous FAD

Enzyme	FAD Ratio (Peak Near 280nm/Peak Near 445nM)
hLCAD Wild Type	8.16
hLCAD Wild Type with FAD	6.64
hLCAD K333Q	12.11
hLCAD K333Q with FAD	9.70

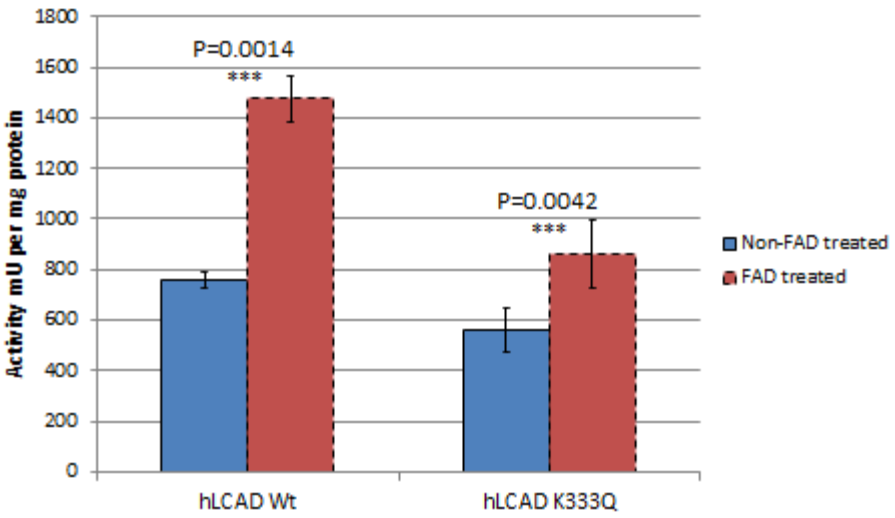

Figure 37: Enzyme Activity Assay of FAD Treated and Non-Treated hLCAD Wt and hLCAD K333Q with C_{16}-CoA

3.2.7 **FAD ratio and enzymatic activity with chemical acetylation.**

Our lab has previously shown that acetylation inhibits the activity of recombinant mLCAD and that this effect maps to lysine residues 318 and 322 (Bharathi S.S., et al. 2013). Specifically, acetylation of K318/K322 shifted FAD in the mLCAD active site, and eliminating the positive charge at these residues caused a loss of FAD similar to that seen in LCAD K333Q. K333Q essentially mimics lysine acetylation by eliminating the positive charge. Therefore, I predicted that the presence of K333Q would exacerbate the negative effects of lysine acetylation at nearby K318 and K322. To test this, wild-type hLCAD and hLCAD K333Q recombinant proteins were chemically acetylated with sulfo-NHs-acetate (SNA) and the resulting effects on function and FAD content were measured. The FAD ratio of both proteins increased following lysine acetylation, indicating a partial loss of FAD, although these changes did not reach statistical significance the wildtype protein shows normal binding of FAD with an FAD ratio near 8, recombinant hLCAD K333Q has an increased FAD ratio of about 9 indicating reduced binding of FAD ($P = 0.055$ and $P = 0.1973$ respectively) (Figure 38). Chemical acetylation significantly reduced the enzymatic activity of hLCAD Wt ($P = 6.05E\text{-}4$) and hLCAD K333Q ($P = 0.011$). The SNP K333Q was even more sensitive to the loss of enzymatic activity with chemical acetylation than recombinant hLCAD Wt ($P = 0.03$) (Figure 39).

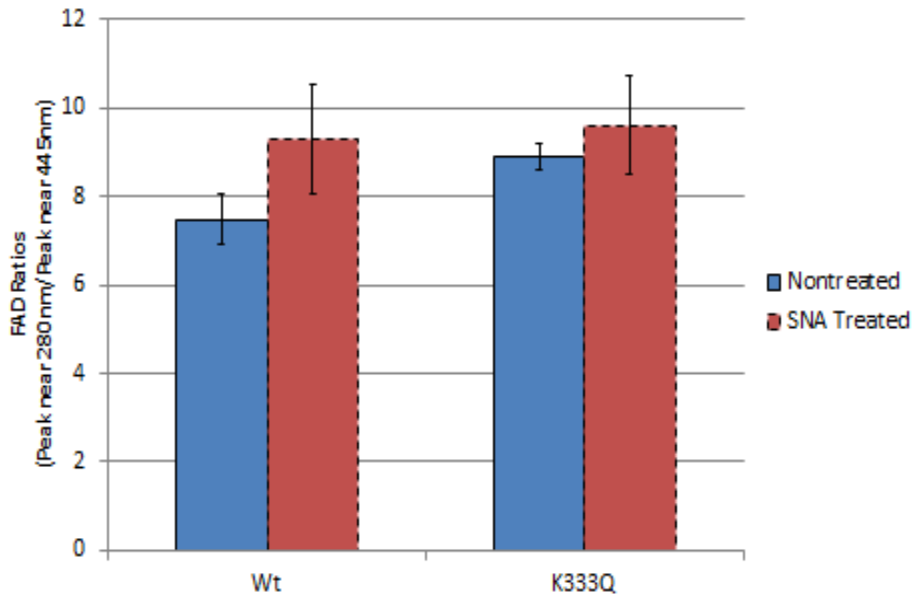

Figure 38: FAD Ratio in Chemically Acetylated and Unacetylated hLCAD Wt and hLCAD K333Q

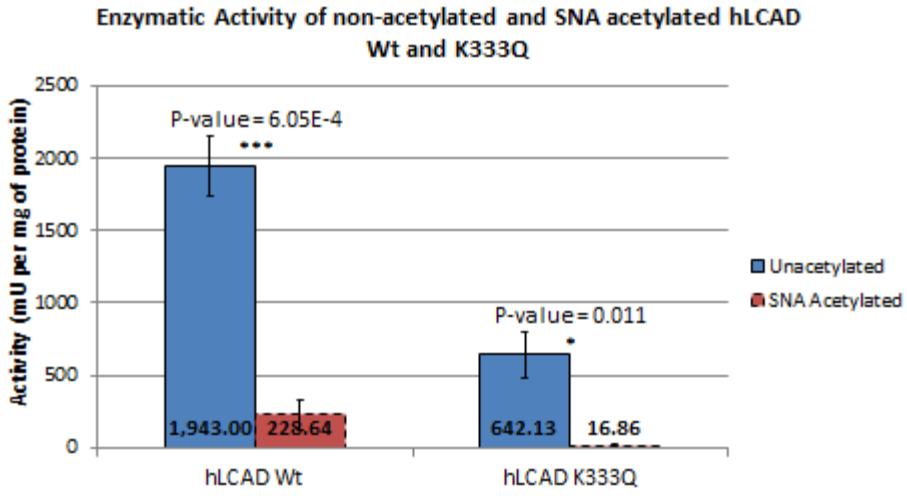

Figure 39: Enzymatic Activity Assay of Chemically Acetylated and Unacetylated hLCAD Wt and hLCAD K333Q with C_{16}-CoA

3.2.8 **Transfected HEK293 cells treated with aspirin.**

Chemical acetylation was shown to reduce the enzymatic activity of hLCAD K333Q. Additionally, acetylation has been shown to regulate mitochondrial proteins (Baeza J., et al. 2016). Therefore, I hypothesized that acetylation may regulate the function of LCAD *in vivo*. An experiment was designed in order to examine the acetylation of human LCAD *in vivo* through the contribution of the acetyl group of acetylsalicylic acid. HEK293 cells were transfected with an hLCAD-Flag expression construct and then treated with 5 mM aspirin. Acetylation of LCAD was determined by immunoprecipitating with anti-Flag followed by western blotting with anti-acetyllysine antibody (Figure 40). Densitometry using the program, Image J, showed that acetylation of LCAD antigen increased approximately 30.3 fold (Figure 41).

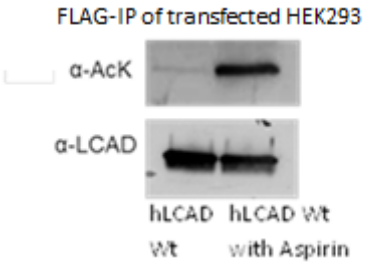

Figure 40: Western Blot of anti-Flag Immunoprecipitation of hLCAD Wt Transfected HEK293 Cells Treated with Aspirin and Untreated

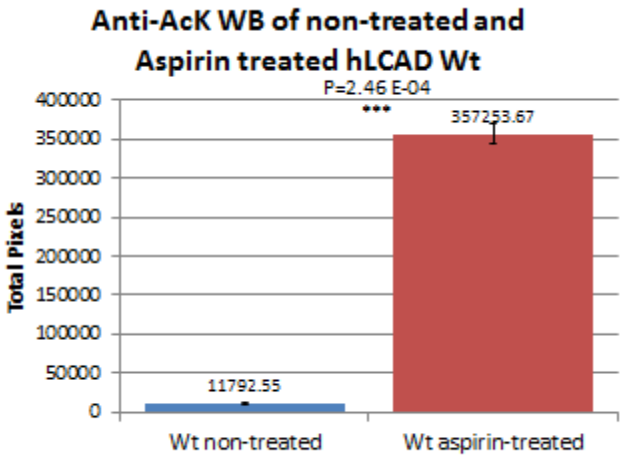

Figure 41: Densitometry of Acetyllysine Antigen in FLAG IP of hLCAD Wt Transfected HEK293 Cells

3.2.9 Acetylation in primary human pneumocytes.

Acetylation was previously shown in our lab to reduce the enzymatic activity of recombinant mouse LCAD (Bharathi S.S., et al. 2013). I additionally showed that chemical acetylation inhibits the enzymatic activity of recombinant human LCAD (Figure 39) and that aspirin acetylates hLCAD Wt *in vivo* (Figure 41). Therefore, I hypothesized that acetylation of LCAD may contribute to the regulation of LCAD in human tissues. In order to examine a possible role of the acetylation of LCAD in human tissues, an experiment was performed to determine whether there is acetylation of proteins occurring in human primary ATII cells where LCAD is known to be highly expressed (Goetzman E.S., et al. 2014). Western blot analysis of 5 µg of primary alveolar type II cell lysates revealed that acetyllysine antigen is indeed present in primary human ATII cells (Figure 42).

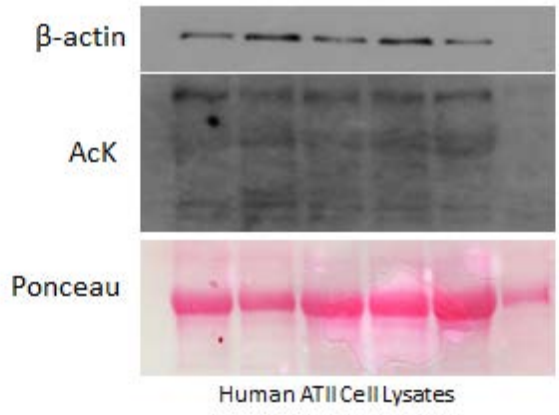

Figure 42: Western Blot of Acetyllysine Antigen in 5 µg of Primary Alveolar Type II Cell Lysates

3.2.10 LCAD in human primary pneumocytes homozygous for the SNP K333Q and homozygous wild type.

Based on my biochemical characterization of recombinant hLCAD K333Q, I hypothesized that the SNP K333Q is detrimental. LCAD is specifically expressed in the ATII cells of the lung in humans (Goetzman E.S., et al. 2014). Therefore, I hypothesized that the SNP K333Q will negatively impact the expression of LCAD in human primary ATII cells. Lysates of primary ATII cells with a known genotype of LCAD K333Q were obtained from collaborators in order to examine the amount of LCAD antigen. The amount of VLCAD and ACAD9 antigen were examined in order to confirm that there was no appreciable expression of ACADs that may compensate for a lack of LCAD. Western blotting of 5µg of primary ATII cell lysates showed significantly reduced LCAD antigen in alveolar type II cell lysates from six people who were homozygous for the SNP, K333Q, as compared to type II cells from six people who were homozygous wild type (Figure 43).

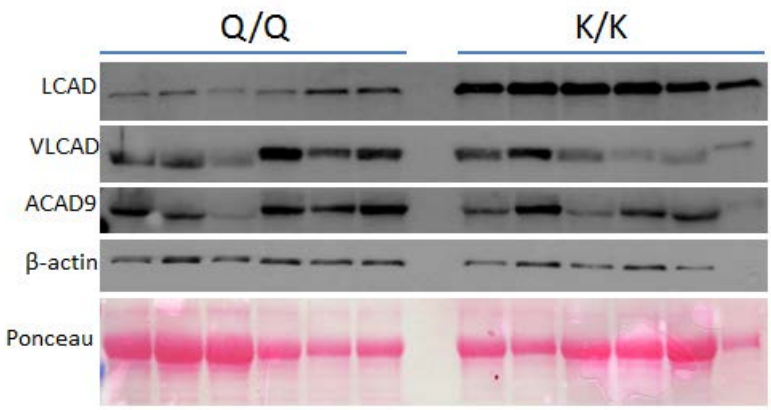

Figure 43: Western Blot of LCAD, VLCAD, ACAD9, and β-actin Antigens in 5 µg of Primary Alveolar Type II Cell Lysates

Densitometry (leaving out the last lane of homozygous wild type due to anomalous protein loading) revealed that LCAD antigen is significantly reduced by about 80% in ATII cells homozygous for the K333Q SNP (Figure 44). VLCAD and ACAD9 antigen were observed in human primary ATII cells upon longer film exposures, and the abundance of these proteins was quite variable. I conclude that while they are present, their abundance is low and they likely would only minimally compensate for any loss of LCAD *in vivo.*

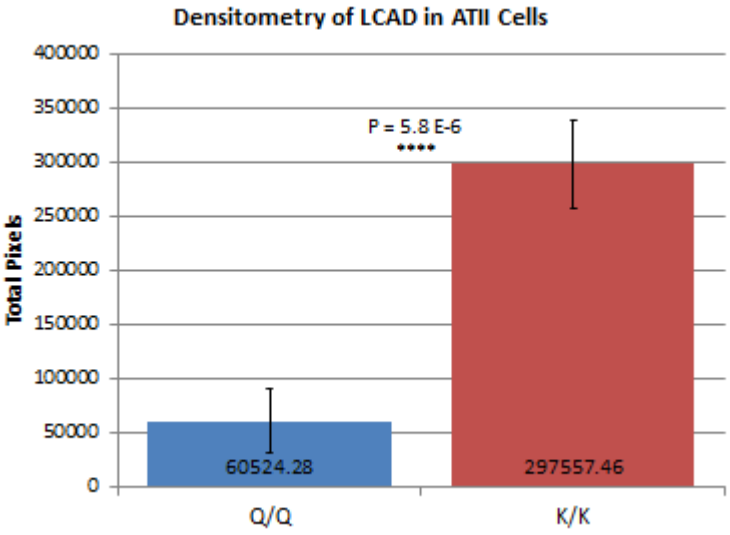

Figure 44: Densitometry of LCAD Antigen in a Western Blot of 5 µg of 6 Human Primary Alveolar Type II Cell Lysates K/K and 5 Q/Q Lysates

3.2.11 Association of SNP K333Q with a lung phenotype.

Based on the observation that K333Q (hereafter the "Q allele") appears to destabilize the hLCAD protein *in vivo*, I hypothesized that a phenotype of LCADD might include a phenotype of lung disease. Furthermore, given that the Q-allele form of SNP K333Q reduced the enzymatic activity of the recombinant enzyme, inhibited the creation of the charge-transfer complex, reduced the stability of the enzyme, and reduced the amount of LCAD antigen, I also hypothesized that the Q-allele would be detrimental and contribute to LCADD. Specifically, I hypothesized that the Q-allele would be associated with decreased lung function or increased risk of lung disease. Therefore, I assessed whether genotypes at SNP K333Q were associated with a variety of lung phenotypes from four different populations:

(1) Lung tissue from lungs not suitable for transplantation (N=149) from Drs. Kosmider and Wang
(2) Caucasian children with respiratory distress syndrome (n= 142) from Dr. Nogee at Johns Hopkins University
(3) Children with pneumonia (n= 775) from Dr. Dahmer at the University of Michigan
(4) Adults from the Long Life Family study (n=4223)

Among the set of 149 lung samples (not suitable for transplantation), genotype frequencies of the three genotypes at SNP K333Q did not differ from the expected frequencies (Table 2; P=0.13). The expected genotype frequencies were based on population allele frequencies of the general population obtained from the 1000 genome project (NCBI. 1000 Genomes Browser, 2013). This result is consistent with *a priori* expectations because the samples were obtained from the general population.

Table 2: K333Q SNP Genotyping of Lungs not Suitable for Transplantation

	Observed	Expected	Chi-Squared
K/K	84	92.7	P-value
K/Q	54	49.6	0.131
Q/Q	11	6.6	
Total	149	149	
	Major Allele Frequency	Minor Allele Frequency	
Allele Freq	0.789	0.211	

Genotype frequencies for SNP K333Q in 142 Caucasian children with respiratory distress syndrome also did not differ from population frequencies, P = 0.33 (Table 3), indicating that the SNP is not associated with respiratory distress, however, the sample size is small.

Table 3: K333Q SNP Genotyping of Children with Respiratory Distress Syndrome

	Observed	Expected	Chi-Squared
K/K	58	60.3	P = 0.334
K/Q	61	64.5	
Q/Q	23	17.2	
Total	**142**	**142**	
	Major Allele Frequency	Minor Allele Frequency	
Allele Freq	0.652	0.349	

The genotyping of SNP K333Q done by Dr. Mary Dahmer in 775 children that were hospitalized for pneumonia also revealed no significant difference in genotype frequencies when the genotype frequencies of children who had additional outcomes of mechanical ventilation (MV), acute lung injury (ALI), and/or asthma were compared by chi-squared to the genotype frequencies of those who did not have an outcome beyond being hospitalized for pneumonia (African American; MV P = 0.976, ALI P = 0.960, and asthma P = 0.987) (Caucasian; MV P = 0.989, ALI P = 0.992, and asthma P = 0.974) (Table 4) (Table 5).

Table 4: K333Q Genotyping of Children (African American) Hospitalized for Pneumonia. A) Children Who Had an Outcome of Mechanical Ventilation B) Children Who Had an Outcome of Acute Lung Injury C) Children Who Had an Outcome of Asthma

A)

Outcome-MV	n	%	MAF
MV=TT	34	79%	
MV=GT	9	21%	0.105
MV=GG	0	0%	
NO MV=TT	305	71%	
NO MV=GT	115	27%	0.159
NO MV=GG	11	2.60%	
Chi-Square			P = 0.976

B)

Outcome-ALI			MAF
ALI=TT	24	83%	
ALI=GT	5	17%	0.086
ALI=GG	0	0%	
NO ALI=TT	315	71%	
NO ALI=GT	119	27%	0.158
NO ALI=GG	11	3%	
Chi-Square			P = 0.960

C)

Outcome-asthma	n	%	MAF
asthma=TT	71	73%	
asthma=GT	22	23%	0.155
asthma=GG	4	4%	
no asthma=TT	268	71%	
no asthma=GT	102	27%	0.154
no asthma=GG	7	2%	
Chi-Square			P = 0.987

Table 5: K333Q Genotyping of Children (Caucasian) Hospitalized for Pneumonia. A) Children Who Had an Outcome of Mechanical Ventilation B) Children Who Had an Outcome of Acute Lung Injury C) Children Who Had an Outcome of Asthma

A)

Outcome-MV	n	%	MAF
MV=TT	21	50%	
MV=GT	14	33.30%	0.333
MV=GG	7	16.70%	
NO MV=TT	132	51%	
NO MV=GT	96	37%	0.305
NO MV=GG	31	12%	
Chi-Square			P = 0.989

B)

Outcome-ALI			MAF
ALI=TT	18	56%	
ALI=GT	10	31%	0.281
ALI=GG	4	12.50%	
NO ALI=TT	135	50%	
NO ALI=GT	100	37%	0.312
NO ALI=GG	34	13%	
Chi-Squared			P = 0.992

C)

Outcome-asthma	n	%	MAF
asthma=TT	21	46%	
asthma=GT	21	46%	0.315
asthma=GG	4	9%	
no asthma=TT	132	52%	
no asthma=GT	89	35%	0.308
no asthma=GG	34	13%	
Chi-Squared			P = 0.974

However, based on allele frequencies from the 1000 genome project there was a significant difference from Hardy-Weinberg Equilibrium in both the Caucasian and African American groups of children hospitalized with pneumonia (Caucasian; P = 5.94E-3 and African American; P = 2.49E-2) (NCBI. 1000 Genomes Browser, 2013). There are more homozygous wildtype than expected (Caucasian; 153 observed and 127.8 expected) (African American; 339 observed and 312.1 expected) and there are fewer heterozygotes than expected (Caucasian; 110 observed and 136.7 expected) (African American; 124 observed and 145.0 expected). In the Caucasian group there are more homozygotes for the Q allele than expected (38 observed and 36.6 expected), whereas in the African American group there are fewer homozygotes for the Q allele (11 observed and 16.8 expected) (Table 6) (Table 7). However, a larger study with controls would need to be done to confirm any difference from Hardy-Weinberg Equilibrium.

Table 6: Hardy Weinburg Equilibrium of Children Hospitalized with Pneumonia (Caucasian)

	Observed	Expected	Chi-Squared
TT	153	127.8	P = 5.94E-3
TG	110	136.7	
GG	38	36.6	
Total	301		
MAF	0.349		

Table 7: Hardy-Weinberg Equilibrium of Children Hospitalized with Pneumonia (African American)

	Observed	Expected	Chi-Squared
TT	339	312.1	P = 2.49E-2
TG	124	145.0	
GG	11	16.8	
Total	474		
MAF	0.189		

In the Long Life Family Study (N=4223), seven lung function traits were tested for association with genotypes at SNP K333Q (rs2286963) overall individuals and by different subgroups.

As can be seen in the LLFS All group (Table 8), individuals with the Q allele had increased lung function, as measured by FEV1 (beta = 29.1, P= 0.019). Furthermore, this improved function in the overall group appeared to be due to the improved function among the controls (beta = 79.0, P = 0.006). These results, however, were not statistically significant given the number of tests performed.

Table 8: Analysis of K333Q (rs2286963) with Measures of Lung Phenotypes in the Long Life Family Study

	All (N = 4223)		Offspring (N = 2323)		Control (N = 734)		Offspring + Control (N = 2891)	
Trait	Beta (SE)	p-value	Beta (SE)	p-value	Beta (SE)	p-value	Beta (SE)	p-value
FEV1	29.1 (12.2)	0.019		0.410	79.0 (28.5)	0.006	33.5 (14.6)	0.024
FEV6	25.7 (14.4)	0.086		0.363	65.2 (34.0)	0.060	33.6 (17.2)	0.061
FEV1/FEV6		0.157		0.582	0.70 (0.00)	0.040		0.107
LungD		0.584		0.682		0.229		0.403
COPD		0.519	-0.17 (0.09)	0.061		0.729		0.190
Asth		0.463		0.964	-0.15 (0.20)	0.092		0.460
Bronch		0.879		0.610	-0.18 (0.97)	0.052		0.582

3.3 ROLE OF LCAD IN THE IMMUNE SYSTEM

3.3.1 Evidence for association of LCAD with the immune system in LCAD -/- mice.

Although my initial hypothesis was that the "Q" allele of SNP K333Q would have a detrimental effect, results from two of the population studies contradict this and may indicate that it actually has a beneficial effect. Therefore, LCAD's natural function may be detrimental in specific environments, such that reducing LCAD activity confers a benefit. One such specific context may be the immune response, which is known to involve bioenergetic switching to facilitate rapid immune cell proliferation (Gerriets V.A., et al. 2015). Additionally, LCAD is expressed in ATII cells which are involved in the innate immune response to inhaled pathogens (Goetzman E.S., et al. 2014) (Crestani B., et al. 1994) (Akgün J., et al. 2015) (Lu R., et al. 2012). Because both mouse and human lung rely predominantly upon LCAD over VLCAD, the LCAD knockout mouse may serve as a useful model to investigate the role of LCAD in the lung (Figure 20). Therefore, LCAD knockout mice (N=4) and wild-type controls (N=5) were infected with influenza by the pathologist Dr. John Alcorn to assess effects on the lung immune response. Dr. John Alcorn then blindly scored the inflammation from 0 being the least inflammation to 4 being the worst. Lungs from LCAD knockout mice showed significantly decreased inflammation as compared to wild type mice (Figure 45) (Figure 46) (Figure 47). Extrapolating to the findings from human cohorts with the Q allele, reduced lung damage as a consequence of reduced inflammation could explain the improved lung function seen in those with the SNP K333Q in the Long Life Family Study.

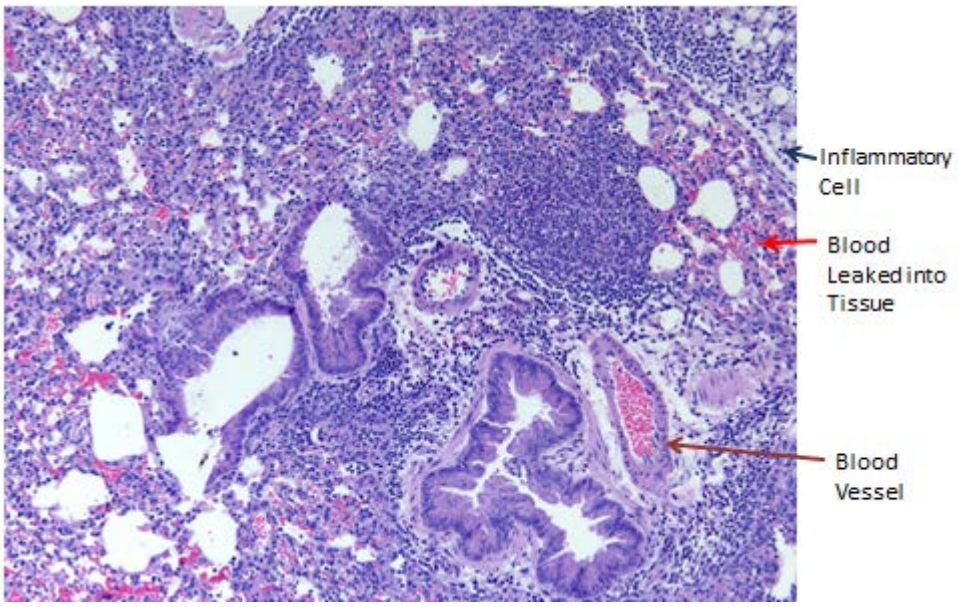

Figure 45: Parenchymal Section of Wild Type Mouse Infected with Influenza

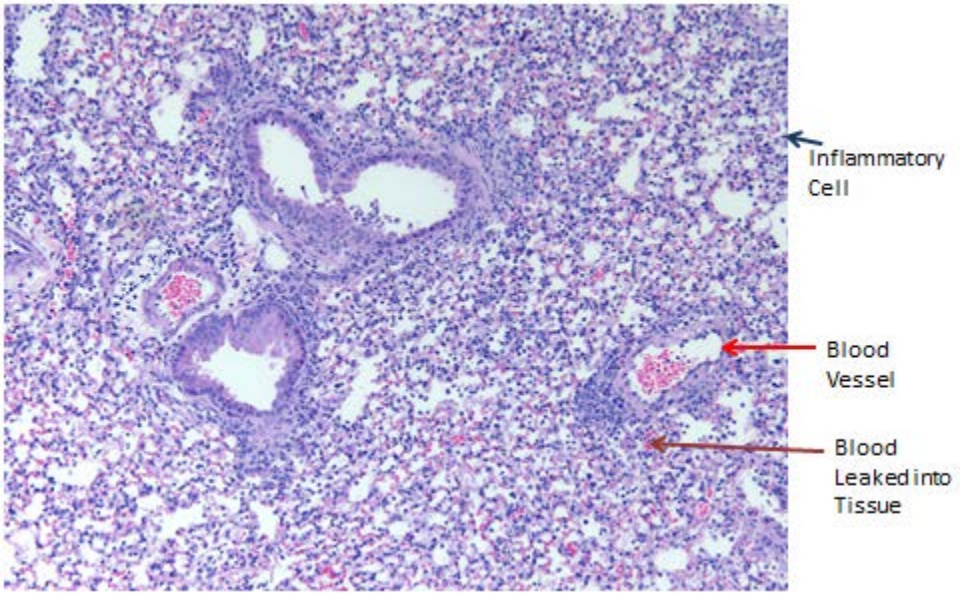

Figure 46: Parenchymal Section of LCAD -/- Mouse Infected with Influenza

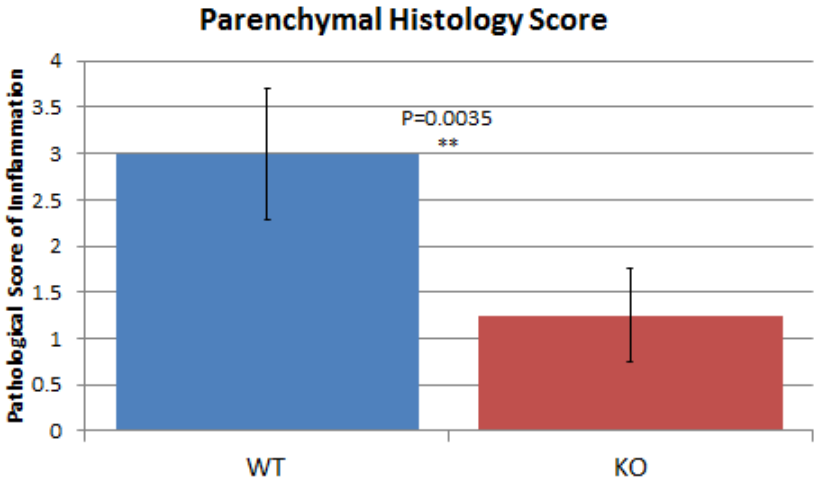

Figure 47: Pathology Scores of Parenchymal Lung Section from 0 (Least Inflammation) to 4 (Highest Inflammation)

3.3.2 Association of the SNP K333Q with the immune system in the LLFS.

To test for a possible association of LCAD with the immune system, three measures of the immune system, including IL-6, white blood cell count, and C-reactive protein, were examined in the Long Life Family Study. Among the Probands, C-reactive protein was increased in individuals who were heterozygous or homozygous for the "Q" allele in SNP K333Q (Table 9; beta = 0.66±0.22, P = 0.004). Thus, individuals with the "Q" allele may have increased levels of inflammation compared to individuals homozygous for the "K" allele (NIH U.S. National Library of Medicine, 2016). However, this effect was only apparent in the Proband generation, and not in the Offspring or the Control Spouses.

Table 9: Analysis of K333Q (rs2286963) with Measures of Immune Phenotypes in the Long Life Family Study

	Proband (n = 1398)		Offspring (n = 2323)		Control (n = 734)		Offspring + Control (n = 2891)		All (n =4207)	
Trait	Beta (SE)	p-value	Beta (SE)	p-value	Beta (SE)	p-value	Beta (SE)	p-value	Beta (SE)	p-value
IL6		0.276		0.870		0.188		0.506		0.864
WBC		0.321		0.158		0.963		0.264	0.07 (0.04)	0.086
CRP	0.66 (0.22)	0.004		0.849		0.843		0.942	0.16 (0.10)	0.095

3.3.3 Surfactant protein-A in mouse lung tissue and bronchial alveolar lavage fluid.

Surfactant protein A (SP-A) is a protein important in the proper function of surfactant (Creuwels L.A., et al. 1997). SP-A is additionally involved in the prevention of damage to surfactant during lung injury (Khubchandani K.R. and Snyder J.M. 2001). Additionally, SP-A is involved in the immune system through the activation of macrophages, the enhancement of the destruction of pathogens in the lung by neutrophils, as well as the suppression of a damaging chronic inflammatory response. SP-A is expressed in ATII where LCAD is expressed in the lung (Creuwels L.A., et al. 1997) (Goetzman E.S., et al. 2014). Therefore, I hypothesized that a lack of LCAD would impact the production of SP-A and impact an immune response. An experiment was designed to examine the possible role of LCAD in the immune system by examining the amount of SP-A antigen in LCAD -/- mice. The western blot showed inaccurate blotting of the first lane of lung tissue lysates of wild type, so it was left out of analysis (Figure 48).

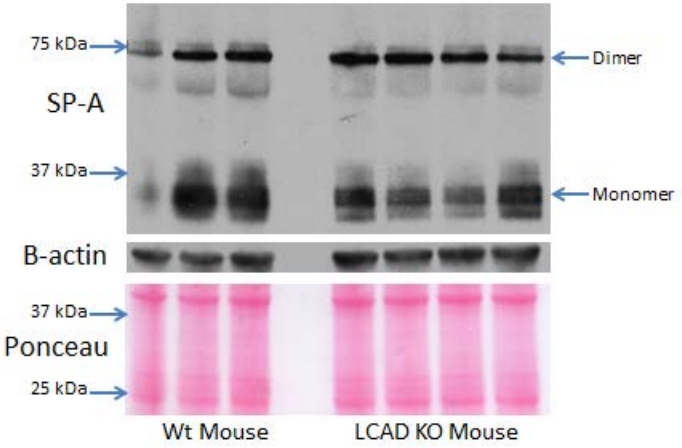

Figure 48: Western Blot of Surfactant Protein-A in 50 µg of Mouse Lung Tissue Lysate

Densitometry with the program, Image J, shows that there is no difference in the dimer form of surfactant protein-A antigen (SP-A) (P = 0.41) (Figure 49). Although, there is significantly less monomer form of SP-A in LCAD KO mice (P = 0.01) (Figure 49).

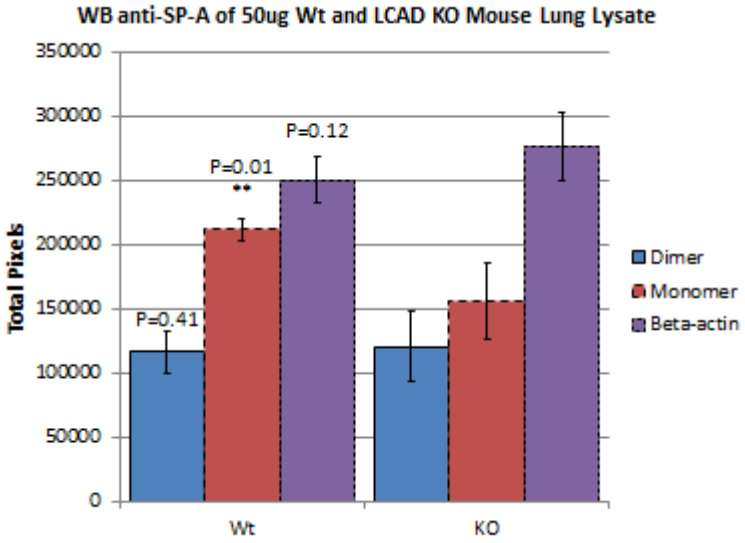

Figure 49: Densitometry with Image J of anti-SP-A Western Blot of 50 µg of Second Two Wild Type and Four LCAD -/- Mouse Lung Lysate

The monomer form is significantly decreased in lung tissue of LCAD KO mice as compared to wild type (P = 0.01) (Figure 49). On the other hand, the monomer form is significantly increased in the BALF of LCAD knockout mice as compared to BALF of wildtype mice (P = 0.032) (Figure 50) (Figure 51).

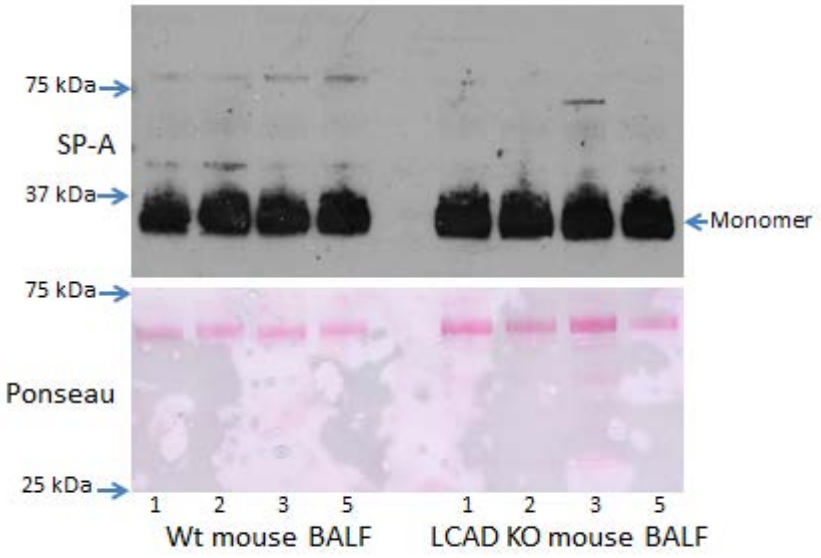

Figure 50: Densitometry with Image J of anti-SP-A Western Blot of 50 µg of Second Two Wild Type and Four LCAD -/- Mouse Lung Lysate

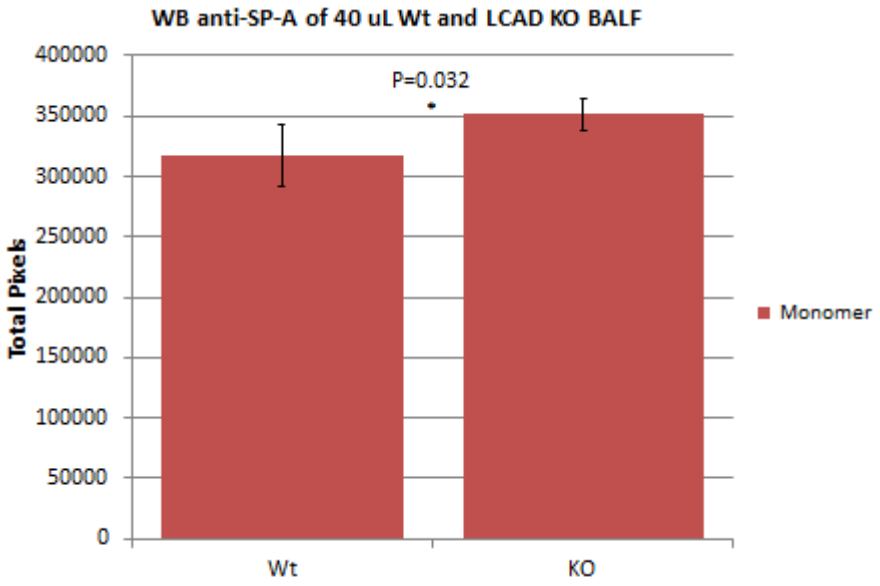

Figure 51: Densitometry with Image J of anti-SP-A Western Blot of 40 µL of Wild Type and LCAD -/- Bronchial Alveolar Lavage Fluid

3.4 CONCLUSIONS

Acetylation has been shown to have a role in the regulation of recombinant LCAD function. Acetylation has been shown to reduce the enzymatic activity of recombinant mouse LCAD at lysines K318 and K322 (Bharathi S.S., et al. 2013). The results of the current study show that acetylation also reduces the enzymatic activity of recombinant human LCAD wild type as well as recombinant human LCAD with the SNP K333Q (Figure 39). In addition, this study shows that aspirin increases acetylation in hLCAD wild type 30.3 fold (Figure 41). Aspirin is well known to trigger metabolic crises in metabolic disorders, particularly in MCAD as well as ACAD9 deficient patients (Green A. and Hall S.M. 1992) (He M., et al. 2007). Furthermore, results of this study showed that acetylation occurs in primary ATII cells where LCAD is

expressed (Figure 42). Therefore, acetylation may be an important regulatory mechanism of LCAD *in vivo* as it has been seen to be here in recombinant protein.

The consequences of the common polymorphism, K333Q, with regards to human health are unknown. However, my results show that K333Q leads to reduced enzymatic activity with the substrates C_{12}-CoA, C_{14}-CoA, C_{16}-CoA, C_{18}-CoA, and $C_{18:1}$-CoA (Figure 23). K333Q reduces the ability of LCAD to bind substrates or to create the charge-transfer complex with the substrates C_{12}-CoA, C_{16}-CoA, and C_{18}-CoA (Figure 26 to 33). K333Q appears to lead to the loss of FAD, which may improve in FAD ratio with the treatment of exogenous FAD (Table 1). Reduced enzymatic activity of K333Q can be partially rescued with exogenous FAD. However, recombinant hLCAD K333Q does not reach the level of enzymatic activity seen with hLCAD Wt (Figure 37). K333Q leads to greater instability with a greater percentage of precipitated protein at 37 ºC than hLCAD Wt (Figure 15) (Figure 34). K333Q also reduces LCAD antigen by about 80% in the primary ATII cells of individuals, homozygous for the SNP as compared to individuals who are homozygous wild type (Figure 44).

The "Q-allele" of SNP K333Q was shown here to be detrimental to recombinant LCAD function. However, children with different genotypes for SNP K333Q shows no differential association with respiratory distress syndrome (Table 3) nor with the outcomes for childhood pneumonia (Tables 4 and 5). On the contrary, the "Q" allele may be beneficial in children hospitalized with pneumonia, as children who were homozygous for the wild type "K allele" were statistically more likely than expected to be hospitalized with pneumonia (Table 6) (Table 7). Although interesting, this analysis needs to be repeated in additional groups. Furthermore, the "Q allele" was associated with increased lung function among spouse controls in the Long Life Family Study, but not among other groups (Table 8).

One possible explanation for the "Q-allele" of SNP K333Q being beneficial *in vivo* is that LCAD is involved in an immune response. SP-A is expressed in the ATII cells where LCAD is expressed, and is involved in the immune response in the lung (Khubchandani K.R. and Snyder J.M. 2001). Western blot of surfactant protein-A in wild-type and LCAD KO mouse lung lysates showed significantly decreased antigen of the monomer form of SP-A in the lung tissue of LCAD KO mice as compared to wild type (Figure 49). On the other hand, there is significantly increased amount of the antigen of the monomer form of SP-A in the BALF of LCAD KO mice as compared to wild type (Figure 51). Therefore, SP-A appears to be increased in the BALF of LCAD KO mice, which does not support an inhibited immune response with the loss of LCAD. On the contrary, C-reactive protein as an indication of inflammation was increased in the proband group of the Long Life Family Study (Table 9). This result may be explained by the report that a decreased ratio of SP-A to surfactant phospholipid is associated with an increased immune response in patients with cystic fibrosis (Khubchandani K.R. and Snyder J.M. 2001). The LCAD -/- mice have abnormally structured and reduced surfactant, and also have increased SP-A antigen in the BALF (Goetzman E.S., et al. 2014). Although LCAD -/- mice infected with influenza had decreased inflammation. Therefore, the association found in patients with CF may not be equivalent to a deficiency of LCAD.

Another possible explanation for the unexpected finding that the "Q-allele" of SNP K333Q may improve the catalytic efficiency of LCAD and the lung function of those with the SNP is that the variant seems to lead to a loss of the cofactor FAD (Table 1). However, when normalized to FAD content, LCAD K333Q has greater catalytic efficiency (Figure 24). Therefore, SNP K333Q may lead to loss of stability and loss of the necessary cofactors LCAD. However, before the enzyme loses the cofactors and falls apart, the SNP K333Q increases

enzymatic activity with the change of the amino acid to a glutamine leading to a change of conformation in the ligand binding sites that increases the enzymatic activity while all parts of the enzyme are still in place.

4.0 SUMMARY

In this study, human LCAD and mouse LCAD were observed to have significantly different levels of enzymatic activity (Figure 8). Human LCAD has significantly less enzymatic activity than mouse LCAD and a lower catalytic efficiency (Figure 9). Thus, the human enzyme is not biochemically equal to the mouse enzyme and may perhaps perform a different function in humans or have an as-yet-undiscovered optimal acyl-CoA substrate. The tissue expression of LCAD also differs between mouse and human tissue lysates (Figure 19). I have confirmed that mouse liver relies heavily upon LCAD for long-chain ACAD activity (Figure 20). Importantly, I report that human hepatocytes express considerable amounts of LCAD, which may explain the absence of liver disease in many patients with VLCAD deficiency (Figure 20). This result also suggests that the deleterious polymorphism K333Q needs to be examined in the context of liver function amongst VLCADD patients.

The enzymatic activity of hLCAD K333Q was reduced compared hLCAD Wt (Figure 23). On the other hand, the catalytic efficiency of hLCAD K333Q was higher than hLCAD Wt (Figure 24). However, the SNP hLCAD K333Q appears to have a loss of FAD (Table 1). FAD is bound between the monomers of LCAD to form the tetramer. Similar to what is reported for isovaleryl-CoA dehydrogenase (IVD), amino acids from two subunits of the LCAD homotetramer bind to the same FAD cofactor (Mohsen A.-W. and Vockley J. 2015). Additionally, analysis of the crystal structure of human LCAD revealed that two amino acids

from a third subunit of the homotetramer, Q328 and H332 bind to FAD (Figure 18). Therefore, each cofactor of FAD is bound by three subunits of the homotetramer of human LCAD. Consequently, the loss of FAD could contribute to the decreased stability seen in hLCAD K333Q (Figure 15) (Figure 34) through the loss of the connections of the monomers and the destabilization of the tetramer. Interestingly, when the loss of FAD is accounted for by normalizing kinetic parameters to FAD content, the mutant K333Q enzyme is more catalytically efficient than its wild type counterpart (Figure 24). But, any kinetic advantage would be outweighed by the loss of protein as was observed in western-blotting experiments of primary ATII cells from those homozygous for SNP K333Q (Figure 43). Finally, small amounts of ACAD9 and VLCAD antigen were seen in human ATII cell lysates (Figure 43). This result requires further investigation, as their presence may compensate for lost LCAD function in the lung and prevent development of an atypical lung phenotype.

APPENDIX: SPECTRA OF STABILITY ASSAY OF RECOMBINANT ENZYME

The spectra of recombinant enzymes mLCAD, hLCAD Wt, and finally hLCAD K333Q which has a glutamine replacing the wild type lysine in all monomers of the pure protein were obtained every 0.5 hours for 2 hours and at 19 hours after incubation on ice, at room temperature, at 37 °C, or at 55 °C.

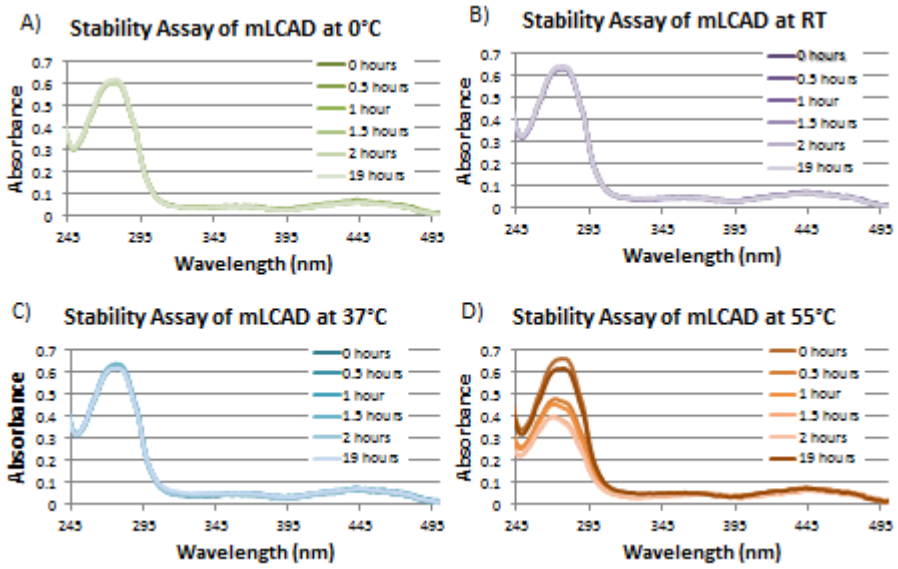

Figure 52: Spectra of the Absorbance from 248 nm to 500 nm of Mouse LCAD Incubated A) On Ice, B) Room Temperature, C) 37°C, D) 55°C for 19 Hours

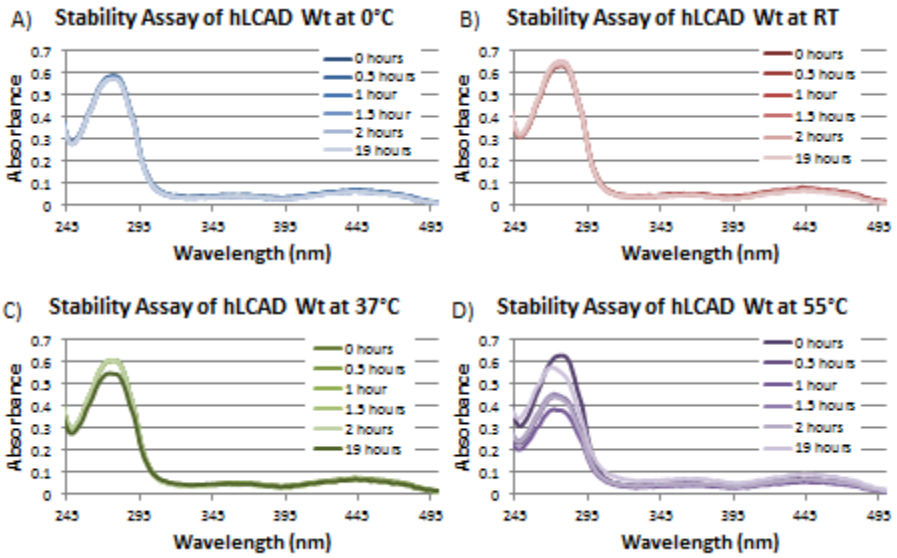

Figure 53: Spectra of the Absorbance from 245nm to 500nm of Human LCAD Wild Type Incubated A) On Ice, B) Room Temperature, C) 37°C, D) 55°C for 19 Hours

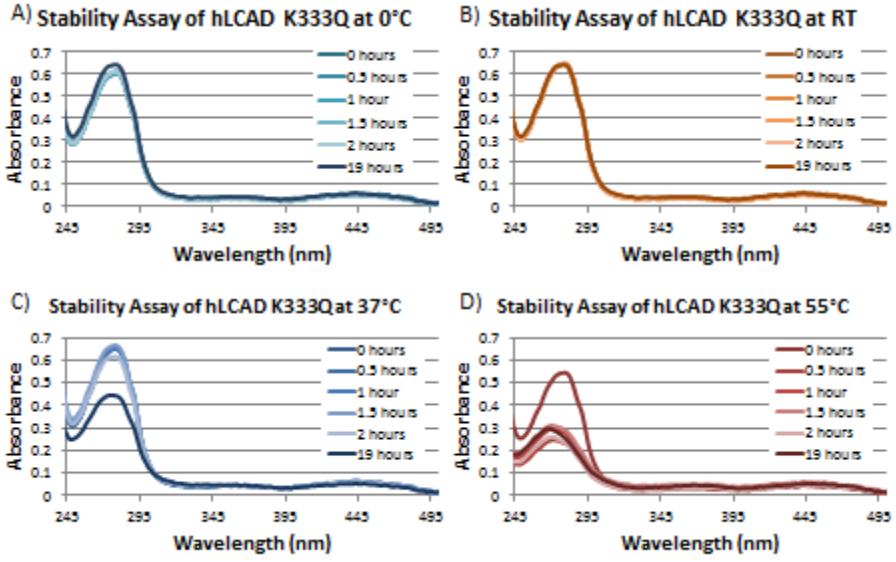

Figure 54: Spectra of the Absorbance from 245nm to 500nm of Human LCAD K333Q Incubated A) On Ice, B) Room Temperature, C) 37°C, D) 55°C for 19 Hours

BIBLIOGRAPHY

Akgün, J., Schabussova, I., Schwarzer, M., Kozakova, H., Kundi, M., Wiedermann, U. (2015). "The Role of Alveolar Epithelial Type II-Like Cells in Uptake of Structurally Different Antigens and in Polarisation of Local Immune Responses." PLoS One. **10**(4):e0124777.

Andresen, B.S., Dobrowolski, S.F., O'Reilly, L., Muenzer, J., McCandless, S.E., Frazier, D.M., Udvari, S., Bross, P., Knudsen, I., Banas, R., Chace, D.H., Engel, P., Naylor, E.W., Gregersen, N. (2001). "Medium-chain acyl-CoA dehydrogenase (MCAD) mutations identified by MS/MS-based prospective screening of newborns differ from those observed in patients with clinical symptoms: Identification and characterization of a new, prevalent mutation that results." Am J Hum Genet. **68**(6): 1408-1418.

Andresen, B.S., Olpin S., Poorthuis B.J.H.M., Scholte, H.R., Vianey-Saban C., Wanders R., Ijlst L., Morris, A., Pourfarzam, M., Bartlett K., Baumgartner E.R., deKlerk J.B.C., Schroeder L.D., Corydon T.J., Lund H., Winter V., Bross P., Bolund L., Gregersen, N. (1999). "Clear Correlation of Genotype with Disease Phenotype in Very-Long-Chain Acyl-CoA Dehydrogenase Deficiency." Am J Hum Genet. **64**(2): 479-494.

Aoyama, T., Souri, M., Ushikubo, S., Kamijo, T., Yamaguchi, S., Kelley, R.I., Rhead, W.J., Uetake, K., Tanaka, K., Hashimoto, T. (1995). "Purification of Human Very-Long-Chain Acyl-Coenzyme A Dehydrogenase and Characterization of Its Deficiency in Seven Patients." J Clin Invest. **95**(6): 2465-2473.

Baeza, J., Smallegan, M.J., Denu, J.M. (2016). "Mechanisms and Dynamics of Protein Acetylation in Mitochondria." Trends Biochem Sci. **41**(3): 231-244.

Banasik, K., Justesen, J.M., Hornbak, M., Krarup, N.T., Gjesing, A.P., Sandholt, C.H., Jensen, T.S., Grarup, N., Andersson, A., Jørgensen, T., Witte, D.R., Sandbæk, A., Lauritzen, T., Thorens, B., Brunak, S., Sørensen, T.I., Pedersen, O., Hansen, T. (2011). "Bioinformatics-Driven Identification and Examination of Candidate Genes for Non-Alcoholic Fatty Liver Disease." PLoS One. **6**(1): e16542.

Berger, P.S., Wood, P.A. (2004). "Disrupted blastocoele formation reveals a critical developmental role for long-chain acyl-CoA dehydrogenase." Mol Genet Metab. **82**(4): 266-272.

Bharathi, S.S., Zhang, Y., Mohsen, A.-W., Uppala, R., Balasubramani, M., Schreiber, E., Uechi, G., Beck, M.E., Rardin, M.J., Vockley, J., Verdin, E., Gibson, B.W., Hirschey, M.D., Goetzman, E.S. (2013). "Sirtuin 3 (SIRT3) Protein Regulates Long-chain Acyl-CoA

Dehydrogenase by Deacetylating Conserved Lysines Near the Active Site." J Biol Chem. **288**(47): 33837-33847.

Chegary, M., Brinke, H.t., Ruiter, J.P., Wijburg, F.A., Stoll, M.S. Minkler, P.E., van Weeghel, M., Schulz, H., Hoppel, C.L., Wanders, R.J., Houten, S.M. (2009). "Mitochondrial long chain fatty acid beta-oxidation in man and mouse." Biochim Biophys Acta. **1791**(8): 806-815.

Cox, K.B., Hamm, D.A., Millington, D.S., Matern, D., Vockley, J., Rinaldo, P., Pinkert, C.A., Rhead, W.J., Lindsey, J.R., Wood, P.A. (2001). "Gestational, pathologic and biochemical differences between very long-chain acyl-CoA dehydrogenase deficiency and long-chain acyl-CoA dehydrogenase deficiency in the mouse." Hum Mol Genet. **10**(19): 2069-2077.

Crestani, B., Cornillet, P., Dehoux, M., Rolland, C., Guenounou, M., Aubier, M. (1994). "Alveolar Type II Epithelial Cells Produce Interleukin-6 In Vitro and In Vivo. Regulation by Alveolar Macrophage Secretory Products." J Clin Invest. **94**(2): 731-740.

Creuwels, L.A., van Golde, L.M. Haagsman, H.P. (1997). "The Pulmonary Surfactant System: Biochemical and Clinical Aspects." Lung. **175**(1): 1-39.

Djordjevic, S., Dong, Y., Pashke, R., Frerman, F.E., Strauss, A.W., Kim, J.-J. (1994). "Identification of the catalytic base in long chain acyl-CoA dehydrogenase." Biochemistry. **33**(14): 4258-4264.

Ensenauer, R., He, M., Willard, J.-M., Goetzman, E.S., Corydon, T.J., Vandahl, B.B., Mohsen, A.-W. Isaya, G., Vockley, J. (2005). "Human acyl-CoA dehydrogenase-9 plays a novel role in the mitochondrial β-oxidation of unsaturated fatty acids." J Biol Chem. **280**(37): 32309-32316.

Exome Variant Server. NHLBI GO Exome Sequencing Project (ESP). (2016) Seattle, WA. http://evs.gs.washington.edu/EVS/

Finocchiaro, G., Ito, M., Tanaka, K. (1987). "Purification and Properties of Short Chain Acly-CoA, Medium Chain Acyl-CoA, and Isovaleryl-CoA Dehydrogenases from Human Liver." J. Biol Chem. **262**(17): 7982-7989.

Fox, I.J., Chowdhury, J.R., Kaufman, S.S., Goertzen, T.C., Chowdhury, N.R., Warkentin, P.I., Dorko, K., Sauter, B.V., Strom, S.C. (1998). "Treatment of the Crigler-Najjar Syndrome Type I with Hepatocyte Transplantation." N Engl J Med. **338**(20): 1422-1426.

Gerriets, V.A., Kishton, R.J., Nichols, A.G., Macintyre, A.N., Inoue, M., Ilkayeva, O., Winter, P.S., Liu, X., Priyadharshini, B., Slawinska, M.E., Haeberli, L., Huck, C., Turka, L.A., Wook, K.C., Hale, L.P., Smith, P.A., Schneider, M.A., Maclver, N.J., Locasale, J.W., Newgard, C.B., Shinohara, M.L., Rathmell, J.C. (2015). "Metabolic programming and PDHK1 control $CD4^+$ T cell subsets and inflammation." J Clin Invest. **125**(1):194-207.

Green, A., Hall, S.M. (1992). "Investigation of metabolic disorders resembling Reye's syndrome." Arch Dis Child. **67**(10): 1313-1317.

Goetzman, E.S. (2011). "Modeling Disorders of Fatty Acid Metabolism in the Mouse." Progress in Molecular Biology and Translational Science. **100**(10): 389-417.

Goetzman, E.S., Alcorn, J.F., Bharathi, S.S., Uppala, R., McHugh, K.J., Kosmider, B., Chen, R., Zuo, Y.Y., Beck, M.E., McKinney, R.W., Skilling, H., Suhrie, K.R., Karunanidhi, A., Yeasted, R., Otsubo, C., Ellis, B., Tyurina, Y.Y., Kagan, V.E., Mallampalli, R.K., Vockley, J. (2014). "Long-chain Acyl-CoA Dehydrogenase Deficiency as a Cause of Pulmonary Surfactant Dysfunction." J Biol Chem. **289**(15): 10668-10679.

Goetzman, E.S., Wang, Y., He, M., Ninness, B.K., Vockley, J. (2007). "Expression and characterization of mutations in human very long-chain acyl-CoA dehydrogenase using a prokaryotic system." Mol Genet Metab. **91**(2): 138-147.

Guerra, C., Koza, R.A., Walsh, K., Kurtz, D.M., Wood, P.A., Kozak, L.P. (1998). "Abnormal nonshivering thermogenesis in mice with inherited defects of fatty acid oxidation." J Clin Invest. **102**(9): 1724-1731.

He, M., Rutledge, S.L., Kelly, D.R., Palmer, C.A., Murdoch, G., Majumder, N., Nicholls, R.D., Pei, Z., Watkins, P.A. Vockley, J. (2007). "A new genetic disorder in mitochondrial fatty acid β-Oxidation: ACAD9 Deficiency." Am J. Hum Genet. **81**(1): 87-103.

Hill, V.K., Ricketts, C., Bieche, I., Vacher, S., Gentle, D., Lewis, C., Maher, E.R., Latif, F. (2011). "Genome-Wide DNA Methylation Profiling of CpG Islands in Breast Cancer Identifies Novel Genes Associated with Tumorigenicity." Cancer Res. **71**: 2988-2999

Hsu, I., Chen, R., Ramesh, A., Corona, E., Kang, H.P., Ruau, D., Butte, A.J. (2013). "Systematic identification of DNA variants associated with ultraviolet radiation using a novel Geographic-Wide Association Study (GeoWAS)." BMC Med Genet. **14**:62.

Illig, T., Gieger, C., Zhai, G., Römisch-Margl, W., Wang-Sattler, R., Prehn, C., Altmaier, E., Kastenmüller, G., Kato, B.S., Mewes, H.W., Meitinger, T., de Angelis, M.H., Kronenberg, F., Soranzo, N., Wichmann, H.E., Spector, T.D., Adamski, J., Suhre, K. (2010). "A genomewide perspective of genetic variation in human metabolism." Nat Genet. **42**(2): 137-141.

Jethva, R., Bennett, M.J., Vockley, J. (2008). "Mini-review: Short-chain acyl-coenzyme A dehydrogenase deficiency." Mol Genet Metab. **95**(4): 195-200.

Khubchandani, K.R., Snyder, J.M. (2001). "Surfactant protein A (SP-A): the alveolus and beyond." FASEB J. **15**(1): 59-69.

Kurtz, D.M., Rinaldo, P., Rhead, W.J., Tian, L., Millington, D.S., Vockley, J., Hamm, D.A., Brix, A.E., Lindsey, J.R., Pinkert, C.A., O'Brian, W.E., Wood, P.A. (1998). "Targeted disruption of mouse long-chain acyl-CoA dehydrogenase gene reveals crucial roles for fatty acid oxidation." Proc Natl Acad Sci U.S.A. **95**(26): 15592-15597.

Le, W., Abbas, A.S., Sprecher, H., Vockley, J., Schulz, H. (2000). "Long-chain acyl-CoA dehydrogenase is a key enzyme in the mitochondrial beta-oxidation of unsaturated fatty acids." Biochim Biophy Acta. **1483**(2-3): 121-128.

Lek, M., Karczewski, K., Minikel, E., Samocha K., Banks, E., Fennell, O'Donnell-Luria, A., Ware, J., Hill, A., Cummings, B., Tukiainen, T., Birnbaum, D., Kosmicki, J., Duncan, L., Estrada, K., Zhao, F., Zou, J., Pierce-Hoffman, E., Cooper, D., DePristo, M., Do, R., Flannick, J., Fromer, M., Gauthier, L., Goldstein, J., Gupta, N., Howrigan, D., Kiezun, A., Kurki, M., Moonshine, A.L., Natarajan, P., Orozco, L., Peloso, G., Poplin, R., Rivas, M., Ruano-Rubio, V., Ruderfer, D., Shakir, K., Stenson, P., Stevens, C., Thomas, B., Tiao, G., Tusie-Luna, M., Weisburd, B., Won, H.-H., Yu, D., Altshuler, D., Ardissino, D., Boehnke, M., Danesh, J., Roberto, E., Florez, J., Gabriel, S., Getz, G., Hultman, C., Kathiresan, S., Laakso, M., McCarroll, S., McCarthy, M., McGovern, D., McPherson, R., Neale, B., Palotie, A., Purcell, S., Saleheen, D., Scharf, J., Sklar, P., Patrick, S., Tuomilehto, J., Watkins, H., Wilson, J., Daly, M., MacArthur, D. (2016). "Exome Aggregation Consortium." Doi: http://dx.doi.org/10.1101/030338

Lu, R., Popov, V., Patel, J., Eaves-Pyles, T. (2012). "Burkholderia mallei and Burkholderia pseudomallei stimulate differential inflammatory responses from human alveolar type II cells (ATII) and macrophages." Front Cell Infect Microbiol. **2**:165.

Maher, A.C., Mohsen, A.-W., Vockley, J., Tarnopolsky, M.A. (2010). "Low expression of long-chain acyl-CoA dehydrogenase in human skeletal muscle." Molecular Genetics and Metabolism. **100**(2):163-167.

Mirkov, S., Myers, J.L., Ramírez, J., Liu, W. (2012). "SNPs Affecting Serum Metabolomic Traits May Regulate Gene Transcription and Lipid Accumulation in the Liver." Metabolism. **61**(11):dio:10.1016/j.metabol.2012.05.004

Moczulski, D., Majak, I., Mamczur, D. (2009). "An Overview of β-Oxidation Disorders." Postepy Hig Med Dosw. **63**:266-277.

Mohsen, A.-W., Vockley, J. (2015). "Kinetic and spectral properties of isovaleryl-CoA dehydrogenase and interaction with ligands." Biochimie. **108**:108-119.

Motyl, K.J., Bishop, K.A., DeMambro, V.E., Bornstein, S.A., Le, P., Kawai, M., Lotinun, S., Horowitz, M.C., Baron, R., Bouxsein, M.L., Rosen, C.J. (2013). "Altered thermogenesis and impaired bone remodeling in Misty mice." J Bone Miner Res. **28**(9):1885-1897.

Nagao M., Tanaka, K. (1992). "FAD-dependent Regulation of Transcription, Translation, Post-translational Processing, and Post-processing Stability of Various Mitochondrial Acyl-CoA Dehydrogenases and of the Electron Transfer Flavoprotein and the Site of Holoenzyme Formation." J Biol Chem. **267**(25):17925-17932.

NCBI. 1000 Genomes Browser: Phase 3. (2013) "Homo sapiens: GRCh37.p13 (GCF_000001405.25) Chr 2(NC_000002.11): 211.1M-21'." http://www.ncbi.nlm.nih.gov/variation/tools/1000genomes/.

NCBI. dbSNP Short Genetic Variations. (2013). "Reference SNP (refSNP) Cluster Report: rs2286963." http://www.ncbi.nlm.nih.gov/SNP/snp_ref.cgi?searchType=adhoc_search&type=rs&rs=rs2286963.

NCBI Protein. (2015). "Acyl-Coenzyme A dehydrogenase, long chain in [Homo sapiens]." Accession: EAW70481. http://www.ncbi.nlm.nih.gov/protein/EAW70481.1.

NCBI Protein. (2006). "Acyl-Coenzyme A dehydrogenase, long chain [Mus musculus]." Accession: AAH27412. http://www.ncbi.nlm.nih.gov/protein/AAH27412.

NIH: NCBI. (2015) "BLAST: blastpsuite. Standard Protein Blast." U.S. National Library of Medicine. http://blast.ncbi.nlm.nih.gov/Blast.cgi?PAGE=Proteins&PROGRAM=blastp&BLAST_PROGRAMS=blastp&PAGE_TYPE=BlastSearch&BLAST_SPEC=blast2seq&DATABASE=n/a&QUERY=&SUBJECTS=.

NIH U.S. National Library of Medicine. (2016). "Medline Plus. C-reactive Protein." https://www.nlm.nih.gov/medlineplus/ency/article/003356.htm.

Papanicolaou, K.N., O'Rourke, B., Foster, D.B. (2014). "Metabolism leaves its mark on the powerhouse: recent progress in post-translational modifications of lysine in mitochondria." Front Physiol. **5**:301.

Parker, A.R. (2003). "Binding of the Human 'Electron Transferring Flavoprotein' (ETF) to the Medium Chain Acyl-CoA Dehydrogenase (MCAD) Involves an Arginine and Histidine Residue." J Enzyme Inhib Med Chem. **18**(5):453-462.

Pike A.C.W., Hozjan, V., Smee, C., Berridge, G., Burgess, N., Salah, E., Bunkoczi, G., Uppenberg, J., Ugochukwu, E., Von Delft, F., Arrowsmith, C.H., Edwards, A., Weigelt, J., Sundstrom, M., Oppermann, U. (2007). "RCSB Protein Data Bank. 2UXW crystal structure of human very long chain acyl-CoA dehydrogenase." http://www.rcsb.org/pdb/explore.do?structureId=2UXW.

Roberts, D.L, Frerman F.E., Kim, J.J. (1996). "Three-dimensional structure of human electron transfer flavoprotein to 2.1-Å resolution." Proc Natl Acad Sci. **93**:14355-14360.

Roberts, J.L., Hovanes, K., Dasouki, M., Manzardo, A.M., Butler, M.G. (2014). "Chromosomal Microarray Analysis of Consecutive Individuals with Autism Spectrum Disorders or Learning Disability Presenting for Genetic Service." Gene. **535**(1):70-78.

Ruzicka F.J., Beinert, H. (1977). "A new iron-sulfur flavoprotein of the respiratory chain. A Component of the fatty acid beta oxidation pathway." J Biol Chem. **252**(23): 8440-8445.

Schiff, M., Haberberger, B., Xia, C., Mohsen, A.-W., Goetzman, E.S., Wang, Y., Uppala, R., Zhang, Y., Karunanidhi, A., Prabhu, D., Alharbi, H., Prochownik, E.V., Haack, T., Häberle, J., Munnich, A, Rötig, A., Taylor, R.W., Nicholls, R.D., Kim, J.-J., Prokisch, H., Vockley, J. (2015). " Complex I assembly function and fatty acid oxidation enzyme activity ACAD9 both contribute to disease severity in ACAD9 deficiency." Hum Mol Genet. **24**(11):3238-3247.

SIFT. (2015). " Sorting Intolerant From Tolerant. SIFT Sequence." http://sift.bii.a-star.edu.sg/www/SIFT_seq_submit2.html.

Souri, M., Aoyama, T., Yamaguchi, S., Hashimoto, T. (1998). "Relationship between structure and substrate-chain-length specificity of mitochondrial very-long-chain acyl-coenzyme A dehydrogenase." Eur J Biochem. **257**(3):592-598.

Swigoňová, Z., Mohsen, A.-W., Vockley J. (2009). "Acyl-CoA dehydrogenases: Dynamic history of protein family evolution." J Mol Evol. **69**(2):176-93.

Tein, I. (2015). "Impact of fatty acid oxidation disorder in child neurology: From Reye syndrome to Pandora's box." Dev Med Child Neurol. **57**(4):304-306.

Tenopoulou, M., Chen, J., Bastin, J., Bennett, M.J., Ischiropoulos, H., Doulias, P.-T. (2015). "Strategies for correcting very long chain acly-CoA dehydrogenase deficiency." J Biol Chem. **290**(16):10486-10494.

Toogood, H.S., van Thiel, A., Basran, J., Sutcliffe, M.J., Scrutton, N.S., Leys, D. (2006). "RCSB Protein Data Bank. 1T9G Structure of the human MCAD:ETF complex." http://www.rcsb.org/pdb/explore.do?structureId=1t9g.

Van Viles, N., Tian, L., Overmars, H., Bootsma, A.H., Kulik, W., Wanders, R.J., Wood, P.A., Vaz, F.M. (2005) "Characterization of carnitine and fatty acid metabolism in the long-chain acyl-CoA dehydrogenase-deficient mouse." Biochem J. **387**(Pt 1):185-193.

Vockley, J., Whiteman, D.A.H. (2002). "Defects of mitochondrial beta-oxidation: a growing group of disorders." Neuromuscul Disord. 235-246.

Wanders, R.J., Vreken, P., den Boer, M.E., Wilburg, F.A., van Gennip, A.H., IJlst, L. (1999). "Disorders of mitochondrial fatty acyl-CoA beta-oxidation." J Inherit Metab Dis. **22**(4): 442-487.

Wang, J., Zhang, C.-J., Zhang, J., He, Y., Lee, Y.M., Chen, S.b., Lim, T.K., Ng, S., Shen, H.-M., Lin, Q. (2015). "Mapping sites of aspirin-induced acetylations in live cells by quantitative acid-cleavable activity-based protein profiling (QA-ABPP)." Sci Rep. **5**:7896.

Wang, Y., Hay, D.C. (2016). "Mass production of stem cell derived human hepatocytes for experimental medicine." Expert Rev Gastroenterol Hepatol. **9**:1-3.

Wilcken, B., Hammond, J., Silink, M. (1994). "Morbidity and mortality in medium chain acyl coenzyme A dehydrogenase deficiency." Arch Dis Child. **70**(5): 410-412.

Xie, B.-X., Zhang, H., Wang, J., Pang, B., Wu, R.-Q., Qian, X.-L., Yu, L., Li, S.-H., Shi, Q.-G., Huang, C.-F., Zhou, J.-G. (2011). "Analysis of Differentially Expressed Genes in LNCaP Prostate Cancer Progression Model." J Androl. **32**(2): 170-182

Yamaguchi, S., Indo, Y., Coates, P.M., Hashimoto, T., Tanaka, K. (1993). "Identification of very-long-chain acyl-CoA dehydrogenase deficiency in three patients previously diagnosed with long-chain acyl-CoA dehydrogenase deficiency." Pediatr Res. **34**(1): 111-113.

Zhang, J., Zhang, W., Zou, D., Chen, G., Wan, T., Zhang, M., Cao, X. (2002). “Cloning and functional characterization of ACAD-9, a novel member of human acyl-CoA dehydrogenase family.” Biochem Biophys Res Commun. **297**(4): 1033-1042.

Zhang, Y., Bharathi, S.S., Rardin, M.J., Uppala, R., Verdin, E., Gibson, B.W., Goetzman, E.S. (2015). “SIRT3 and SIRT5 Regulate the Enzyme Activity and Cardiolipin Binding of Very Long-Chain Acyl-CoA Dehydrogenase.” PLoS One. **10**(3):e0122297.